DETERMINATION OF SUBGRADE STRENGTH UNDER INTACT PORTLAND CEMENT CONCRETE SLABS FOR RUBBLIZATION PROJECTS

Final Report
(Report No. FHWA/NC/2002-010)

To North Carolina Department of Transportation
(Research Project No. HWY-1999-02)

Submitted by

Y. Richard Kim, Ph.D., P.E.
Campus Box 7908
Department of Civil Engineering
North Carolina State University
Raleigh, NC 27695-7908
Ph: 919-515-7758
Fax: 919-515-7908
E-mail: kim@eos.ncsu.edu

Sungho Mun
Graduate Student

May 2002

Technical Report Documentation Page

1. Report No. FHWA/NC/2002-010	2. Government Accession No.	3. Recipient's Catalog No.
4. Title and Subtitle Determination of Subgrade Strength under Intact Cement Concrete Slabs for Rubblization Projects		5. Report Date May 21, 2002 6. Performing Organization Code
7. Author(s) Y. Richard Kim and Sungho Mun		8. Performing Organization Report No.
9. Performing Organization Name and Address North Carolina State University Department of Civil Engineering Campus Box 7908 Raleigh, NC 27695-7908		10. Work Unit No. (TRAIS) 11. Contract or Grant No.
12. Sponsoring Agency Name and Address North Carolina Department of Transportation Research and Analysis Group 1 South Wilmington Street Raleigh, NC 27601		13. Type of Report and Period Covered Final Report July 1998 - June 2000 14. Sponsoring Agency Code 1999-02
15. Supplementary Notes		

16. Abstract

Rubblization is an effective rehabilitation method for deteriorated Portland cement concrete (PCC) pavements due to its low initial cost, minimum traffic disruption, and ability to minimize reflective cracking in asphalt overlays. However, the loss of strength in PCC slab due to rubblization creates the demand for a subgrade that is strong enough to handle traffic after rubblization. AASHTO recommends Falling Weight Deflectometer (FWD) testing of PCC pavements before rubblization to ascertain the subgrade strength after rubblization. However, the existing deflection analysis methods do not adequately handle the change in stress states in the subgrade before and after rubblization, and therefore result in erroneous prediction of subgrade strength. The primary objective of this study is to develop an analysis method that allows the realistic estimation of subgrade strength after rubblization from deflection measurements on intact PCC slabs before rubblization. As a forward model, stress/strain dependent nonlinear subgrade models were incorporated into a finite element analysis. ABAQUS and NCPAVE, a finite element code developed at North Carolina State University, were used in the analysis. Multi-load FWD testing was conducted in the field to generate varying stress states in the subgrade under intact PCC pavements. Based on the synthetic database generated from the finite element analyses, a number of relationships were developed using regression and Artificial Neural Network (ANN) approaches to predict the coefficients in the nonlinear subgrade model from multi-load FWD deflections. The verification study was performed on the resulting algorithms using limited field data derived from US 29 in Guilford County and I-85 in Rowan County. The research suggests that the stress-based regression approach, which determines the nonlinear coefficients by regressing between the subgrade moduli and stresses predicted at several radial distances from the FWD load from multi-load deflections, is the most promising method of analysis. The research team strongly recommends the further verification of this procedure using additional field data before the implementation.

17. Key Words Rubblization, Subgrade Strength, Falling Weight Deflectometer, PCC Pavement, Multi-Load FWD, Nonlinear Behavior of Subgrade	18. Distribution Statement		
19. Security Classif. (of this report) Unclassified	20. Security Classif. (of this page) Unclassified	21. No. of Pages 115	22. Price

Form DOT F 1700.7 (8-72) **Reproduction of completed page authorized**

ABSTRACT

Rubblization is an effective rehabilitation method for deteriorated Portland cement concrete (PCC) pavements due to its low initial cost, minimum traffic disruption, and ability to minimize reflective cracking in asphalt overlays. However, the loss of strength in PCC slab due to rubblization creates the demand for a subgrade that is strong enough to handle traffic after rubblization. AASHTO recommends Falling Weight Deflectometer (FWD) testing of PCC pavements before rubblization to ascertain the subgrade strength after rubblization. However, the existing deflection analysis methods do not adequately handle the change in stress states in the subgrade before and after rubblization, and therefore result in erroneous prediction of subgrade strength.

The primary objective of this study is to develop an analysis method that allows the realistic estimation of subgrade strength after rubblization from deflection measurements on intact PCC slabs before rubblization. As a forward model, stress/strain dependent nonlinear subgrade models were incorporated into a finite element analysis. ABAQUS and NCPAVE, a finite element code developed at North Carolina State University, were used in the analysis. Multi-load FWD testing was conducted in the field to generate varying stress states in the subgrade under intact PCC pavements. Based on the synthetic database generated from the finite element analyses, a number of relationships were developed using regression and Artificial Neural Network (ANN) approaches to predict the coefficients in the nonlinear subgrade model from multi-load FWD deflections. The verification study was performed on the resulting algorithms using limited field data derived from US 29 in Guilford County and I-85 in Rowan County. The research suggests that the stress-based regression approach, which determines the nonlinear

coefficients by regressing between the subgrade moduli and stresses predicted at several radial distances from the FWD load from multi-load deflections, is the most promising method of analysis. The research team strongly recommends the further verification of this procedure using additional field data before the implementation.

DISCLAIMER

The contents of this report reflect the views of the authors and not necessarily the views of the University. The authors are responsible for the facts and the accuracy of the data presented herein. The contents do not necessarily reflect the official views or policies of either the North Carolina Department of Transportation or the Federal Highway Administration at the time of publication. This report does not constitute a standard, specification, or regulation.

ACKNOWLEDGMENTS

The authors would like to acknowledge the support of the North Carolina Department of Transportation and the Federal Highway Administration. Special thanks go to engineers in the Pavement Management Unit for their help in FWD testing.

TABLE OF CONTENTS

LIST OF TABLES

LIST OF FIGURES

CHAPTER ONE
INTRODUCTION

According to the National Asphalt Pavement Association (NAPA), there are approximately 500,000 lane miles of Portland cement concrete (PCC) pavement within the United States highway system (PCS, 1991). About one-half of these pavements comprise the current Interstate System. There are many techniques currently used to rehabilitate these aging PCC pavements. The majority of the techniques commonly used today incorporate either an asphalt concrete (AC) or PCC overlay. Among the most popular is a simple surface course overlay using hot-mix asphalt to restore surface rideability and integrity. The major problem of AC overlay over PCC slabs is the recurrence of cracks in the rehabilitated surface layer, known as reflective cracking. In order to retard the reflective cracking, one may think that an overlay thickness may be increased. However, according to Corley-Lay (1995), Indiana DOT reported "thicker overlays increased construction costs but did not reduce long term reflective cracking."

Several rehabilitation techniques have been developed to deal with reflective cracking in overlays on PCC pavement (refer to Chapter 2). Since the late 80's, a new technique called *rubblization* has received increasing attention as a viable solution to minimize reflective cracking in overlays on PCC pavement. The technique involves destroying the existing PCC slab into pieces smaller than one foot in order to provide an improved base material for the future overlay. In this manner, the deteriorated PCC pavement is essentially converted to a high-strength granular base and gives the appearance of an unbound base material as in AC pavement construction.

According to the NAPA report (PCS, 1991), rubblization is most suitable for cases where PCC slabs have deteriorated to a point where there is little potential of significant slab integrity or structural capacity using other rehabilitative techniques. They add, however, that rubblizing appears to be equally effective for all types of PCC pavement types and that it is actually the preferred method when any type of slab reinforcement is present. A preliminary investigation for the Wisconsin Department of Transportation (Nelson and Owusu-Ababio, 1994) concluded, "rubblization techniques have been successfully used on PCC pavements exhibiting punchouts, delaminations, patching, and cracking in both the longitudinal and transverse directions."

Given the relatively short time period since the rubblization was first introduced in 1986 (Schackner, 1989), there is not a very strong database of information to adequately gauge the performance of the rubblized sections. However, preliminary investigations tend to indicate that the vast majority of the rubblized pavements are performing well with respect to reflection crack control, rideability, etc. Also, the rubblization technique results in lower initial cost and minimum disruption of traffic and safety-related problems due to accelerated construction.

NCDOT also had success in the first rubblization project on I-95 in Northhampton County. Since then, NCDOT has used the rubblization technique in several major projects, including I-440 beltline around Raleigh, I-85 North of Durham, and NC-26 near Beulahville. However, the experience of NCDOT in these rubblized projects results in a mixed feeling due to inaccurate estimation of subgrade strength before rubblization (refer to Section 1.2).

For the rubblization project to be successful, it is important to have a subgrade that is strong enough to handle the traffic after the PCC layer loses its strength due to rubblization. AASHTO recommends deflection testing of the pavement (ASTM D 4694 and D 4695) in order to better ascertain its structural properties (AASHTO, 1993). This testing is normally accomplished using a heavy-load deflection device such as a Falling Weight Deflector (FWD) and measuring the pavement response in terms of deflection. The FWD tests provide some insight into the structural capacity of the pavement and base layer(s) or subgrade before rehabilitation. If the results of the deflection tests prove to be unsatisfactory or, if the tests are not used at all, AASHTO recommends coring and material testing of the deteriorated pavement. It is also recommended that deflection tests be performed on the fractured slabs after rubblization to confirm the structural capacity of the resultant structure. To date, there is no accepted method to directly correlate pre- and post-rubblization moduli of subgrade.

The NCDOT has experienced significant differences in backcalculated moduli on a recent project on I-85 North of Durham (Corley-Lay, 1997). The effect of this variability in backcalculated moduli for rubblized sections can be potentially very costly and timely. For example, if a certain subgrade is believed to be stronger than post-rubblization tests reveal, it may be necessary to abort rubblization, undercut the rubblized sections and proceed with a full-depth pavement design and construction. DOTs, contractors, and taxpayers are obviously very eager to be able to ascertain the condition of the pavement structure before rehabilitation contracts are let out for bid.

Rubblization as a rehabilitative technique has continually proved to be an effective method for managing aged and deteriorated PCC pavements due to appealing performance and the recent advancements in equipment technology. To fully take advantage of this technique, North Carolina Department of Transportation has funded a two-year research project "Determination of Subgrade Strength under Intact Portland Cement Concrete Slabs for Rubblization Projects." This report presents the findings from the project and the recommended procedure for estimating subgrade modulus under rubblized PCC slabs from FWD deflections measured on PCC pavements prior to rubblization.

1.1 Research Objective and Report Organization

The primary objective of this research is to develop an analysis method that enables the estimation of subgrade modulus after rubblization from deflection measurements on intact PCC slabs before rubblization. To accomplish this objective, nonlinear behavior of subgrade under multi-level FWD loads was investigated using finite element analysis. Several backcalculation (or so-called inversion) algorithms were evaluated as the vehicle to predict the subgrade condition from measured deflections. Findings from this research will be presented in seven chapters in this report, and the brief description of each chapter is given below.

Chapter 2 presents a literature review on the rehabilitation techniques of PCC pavements and nonlinear models of subgrade. The understanding of nonlinear behavior of subgrade soils is essential for predicting post-rubblization subgrade moduli from deflections measured from PCC slabs before rubblization. Both stress and strain based

nonlinear models are presented. Chapter 3 introduces the finite element analysis used in this study to incorporate the nonlinear model of subgrade. Chapter 4 presents the details involved in developing several subgrade condition evaluation algorithms. These algorithms are evaluated in Chapter 5 using limited field data, and the recommendation is made based on the comparison of their performance. Chapter 6 provides the conclusions of the study as well as future research direction in this research area. Various backcalculation algorithms for subgrade modulus are briefly summarized in Appendix A.

1.2 Rubblization in North Carolina

Since its inception, rubblization has been used on many projects throughout the United States. A brief discussion of some rubblized projects across the nation is given below, followed by case studies in North Carolina.

The first known project to use rubblization was Route 146 in Clifton Park, NY around 1986 (Schackner, 1989). The Route 146 project was a two-mile stretch which was to be used as a test program for the larger, upcoming Route 7 project. The result of using rubblization cut the project price tag in half along with increasing the expected design life of the roadway. In 1990, an eight to nine inch concrete pavement was rubblized on I-59 in Laurel, MS with appreciable success (Kuennen, 1991). During the same year, a section of I-77 in West Virginia was successfully rubblized (Kuennen, 1991). In an experimental roadway section of I-35 (Southbound) in Kay County, Oklahoma, rubblization was compared side-by-side against other fracture techniques. Daleiden *et al.* (1995) reported results from this project as follows: “When comparing the current condition of each test section with the others, it is apparent that the rubblized test

sections are outperforming the other test sections." The PCS study (PCS, 1991) also concluded that "the lower the Epcc value (or the smaller the slab size), the greater the effectiveness of the construction operation in minimizing the potential for eventual reflective cracking in the HMA overlay."

A 1995 article in Michigan Contractor and Builder (Bloemendaal, 1995) highlighted a rubblization project on Cascade Road in Kent County, MI. The project was a 2.2 mile section and the scope of work included cold milling of an existing overlay, rubblizing, and the subsequent placement of a bituminous overlay. The first rubblization project in the southeast US was a 9.4-mile stretch of I-77 near Columbia, SC. The project, which was strongly backed by FHWA, was performed during late 1988 and was delivered at approximately $5.4M. The South Carolina Department of Highway and Public Transportation reportedly viewed the project as a success and stated that they would consider the technique on other projects in the future.

North Carolina first used rubblization on I-95 in Northhampton County around 1990 (Corley-Lay *et al.*, 1995). The project was constructed as a comparison to then-popular crack and seat projects. Prior to testing the sections side-by-side, engineering opinion within NCDOT was not uniform on either technique. "One engineer was a strong proponent, arguing the significant cost savings for traffic control when crack and seat is used instead of rubblization. Another was adamantly opposed, feeling that you lose favorable bridging effects and end up with rocking slabs using crack and seat" (Corley-Lay *et al.*, 1995). Both types of sections were exposed to over one million equivalent single axle loads. Reportedly, no pavement distress of any kind was found on the rubblized section of I-95.

NCDOT has since used rubblization on a section of the I-440 beltline around Raleigh, I-85 North of Durham, and NC-26 near Beulahville. Rubblization of the I-440 beltline was chosen as an attractive technique both from a cost and traffic control standpoint. According to an article in Asphalt magazine (Waller), the beltline sustains average daily traffic of more than 100,000 vehicles with about two percent trucks and poses the potential for a major bottleneck. The rubblization and overlay of the 3.6-mile segment was part one of a three stage venture and was worth about $21.5M. At the completion of this stage, Steve DeWitt, NCDOT Resident Engineer, stated that the project went well and that NCDOT intends to continue using rubblization for the next stage of the beltline project (Waller). Incidentally, the I-440 segment was awarded a National Quality Initiative Award, and local contractor C.C. Mangum was also honored for their work.

In spite of these successes, the I-85 and NC-26 rubblization projects exhibited less than satisfactory results. Because of the inconsistency of results when rubblization is used, there is not complete agreement on its recommended use for future projects.

The NC 26 roadway was a thin, 6.5-inch, unreinforced slab which rested on basically raw subgrade and was also more than 30 years old. Based upon the thickness of the pavement and the condition of the subgrade, NCDOT did not expect stellar results from this section, but hoped to learn more about the nature of rubblizing from the experience in order to analyze its applicability to some other upcoming projects around the state. As it turned out, NCDOT's predictions were correct, and the rubblized section of NC 26 project had to be undercut.

The I-85 project (Corley-Lay, 1996), was not expected to be a problematic project. During the rehabilitation of the northbound lane from south of Red Mill Road to north of Red Wood Road, NCDOT resident engineer, Tracy Parrott, reported seeing conditions after rubblization which could potentially affect the desired performance of the rehabilitated pavement. Based upon these concerns, the NCDOT conducted FWD tests on the rubblized and overlaid portions of the northbound lane. The tests indicated that the overlain pavement exhibited "very poor subgrade support and deflections that are too high to sustain the traffic loads projected for a ten year pavement life."

Recommendations for the northbound lanes included full-depth repair of some previously rubblized sections and overlay on some unrubblized sections. The overlay was suggested based on the satisfactory performance observed from an overlain section immediately south of the project which had been exposed to similar traffic. Undercut depths for the rubblized portions of the northbound lanes ranged from two to seven feet. To date, the project is about 60% complete and according to Kevin O'Dell, NCDOT Resident Engineer, the total overruns on the rubblized portions of I-85 currently equate to a cost of about $427,000. This figure included costs associated with undercutting (~$219,000) and additional heavy-duty surface and binder (~$208,000) but still does not accurately reflect the real costs of the change order. The real costs would include such things as time delays of the contractor and subcontractors, redesign by DOT, scheduling adjustments by the contracting parties, equipment mobilization/demobilization, and other intangibles such as lost work time of commuters due to traffic delays, etc. It was also noted in other NCDOT correspondence that, although reflective cracking is expected to

appear within a two-year period, the overlain pavement should be able to meet the desired 10-year life.

In light of the situation on the northbound portion of the I-85 project, NCDOT Pavement Management Unit (PMU) advised that testing of the southbound lanes before and after rubblization might be useful, although they were not certain that poor subgrade conditions could be detected on intact slabs due to the "spreading" of the imposed load from the FWD over a large area. Corley-Lay *et al.* (1995) reports that backcalculated modulus values for rubblized concrete is in the range of 200 to 700 ksi and that decreasing the crack spacing (from break and seat to rubblization, for instance) decreases the PCC slab modulus, Epcc, and the subgrade modulus.

Additionally, the PMU engineers recommended that NCDOT would like to test the rubblized sections of the southbound lane and that they have some flexibility in adjusting overlay designs accordingly. Testing of the southbound lane before rubblization revealed subgrade resilient modulus values ranging from 12,500 to 27,000 psi. After rubblization, subgrade resilient modulus values were found to lie in the 3,000 to 10,000 psi range. At one test location (near station 585+00), the modulus was measured to be about 27,000 psi before rubblization and about 6,000 psi after rubblization. Of the rubblized sections which were tested on the southbound lane, all were found to be below the acceptable subgrade strength level required for overlay. These types of discrepancies are not allowable. The state DOTs would obviously like to be able to predict the structural capacities of the base and subgrade layers of pavements before rehabilitation design and contract letting. Not only are the costs of undercutting

and redesign of pavements very high, the sunken costs of the previously rubblized pavements are equally disturbing.

CHAPTER TWO
LITERATURE REVIEW

There are various rehabilitation techniques for deteriorated PCC pavements today, of which the most popular is the asphalt overlay. One of the major problems with this technique is the reflective cracking from existing PCC slabs. To retard the reflective cracking, several different techniques have been developed and used widely in the United States. The selection of rehabilitation strategy depends on the condition and type of PCC pavement. This chapter first reviews different rehabilitation methods used along with asphalt overlay over PCC pavements. The second part of the chapter reviews various models describing the nonlinear behavior of subgrade soils, of which understanding is essential for estimating the change in subgrade modulus due to breaking PCC slabs.

2.1 PCC Rehabilitation Techniques

2.1.1 Saw and Seal

This technique is used to reduce reflected cracking due to thermal cycling in PCC slab. In this technique, joints in PCC slabs are sawed and sealed with polymers. The sawing width is approximately one to two inches in the shape of straight and narrow cracks to make the sealing easier. However, Hylton (1997) reported "Saw and seal could be used for both Jointed Concrete Pavement (JCP) and Jointed Reinforced Concrete Pavement (JRCP), but the joint spacing on most JCP is so short that it makes the cost of saw and seal impractical." He also suggested that saw and seal technique with a thick AC overlay could perform better than that with a thin AC overlay.

2.1.2 Crack/Seat and Break/Seat

Crack and seat and *break and seat* methods have been employed to reduce the effective slab length of PCC pavements primarily to lessen or potentially eliminate the stresses on the overlay associated with thermal cycling of the slab. The 1993 AASHTO Guide about the crack/seat method states that Jointed Reinforced Concrete Pavements (JRCP) should typically be broken into pieces one to three feet in size and be seated firmly into the foundation. Additionally, the AASHTO (1993) mentions that the break/seat consists of breaking a JRCP into pieces lager than about one foot, rupturing the reinforcement or breaking its bond with the concrete, and seating the pieces firmly into the foundation. These techniques are to be used with JRCP to reduce the size of PCC pieces to minimize the differential movements at existing cracks and joints.

2.1.3 Rubblization

The technique of rubblization is to completely fracture any type of PCC slab into pieces into smaller than one foot and then to firmly compact the layer, typically with a resonant frequency concrete breaker or a badger breaker. Thompson (1999) describes that "a rubblized and compacted PCCP (Portland Cement Concrete Pavement) is an assemblage of PCC segments that form a tightly keyed/interlocked and high density material layer, and it posses high shear strength and rutting resistance." Furthermore, The research performed by Thompson (1999) showed that excellent performance was achieved on the Pesotum project which has accommodated approximately 7.5 million ESALs (Equivalent Single Axle Loads) through the summer of 1998.

Figure 2.1 shows a resonant frequency breaker operating on US 29, and Figure 2.2 shows rubblized concrete. The resonant frequency breaker gives a low amplitude (0.5 in or 13 mm) and a high frequency resonant energy delivered to the PCC slab, and causes a high tension at the surface (Niederquell *et al.,* 2000).

Figure 2.1 Resonant frequency breaker

Figure 2.2 Rubblized concrete by resonant frequency breaker

2.2 Stress-State Dependent Subgrade Models

The theory of linear elasticity has been widely used to describe the behavior of subgrade soil in pavement structure. Whether a more complicated nonlinear model is necessary or not depends on the nature of the problem. For example, the analysis of intact PCC pavements under typical highway traffic does not require a nonlinear model for subgrade (Kim, 2000). However, when the PCC slab is broken, the same load increases stresses in subgrade and nonlinear subgrade models may be more warranted. In general, stresses in unbound layers in pavements are underestimated for these layers when the linear elastic model is employed for these layers. Additionally, Ullidtz (1998) described the importance of the nonlinear analysis in subgrade layer. It is found that the intermediate granular layer having a lower modulus than the subgrade when a linear elastic subgrade in a backcalculation was taken. Quite a few nonlinear models have been

suggested by researchers. In this chapter, these models are briefly described for granular and fine-grained soils.

2.2.1 Granular Soil

The resilient modulus in granular materials has been known to be stress-state dependent. Several models have been developed for analyzing the characteristics of granular materials.

The $k-\theta$ model has been the most popular in representing the stress-state dependency of granular materials. The resilient modulus is expressed as a function of the bulk stress as follows:

$$M_r = k_1 \theta^{k_2} \tag{2.1}$$

where

M_r = resilient modulus,

θ = bulk stress ($=\sigma_1 + \sigma_2 + \sigma_3$), and

k_1, k_2 = regression constants determined from the repeated triaxial loading test results.

The contour model proposed by Brown and Pappin (1981) expressed the shear and volumetric stress-strain relations for granular materials using the stress path to simulate the actual pavement conditions. Due to the complication of the contour model, it is difficult to use it as a practical model in characterizing granular materials. Brown and Pappin also emphasized the importance of effective stress, which is influenced by pore pressure in partially or totally saturated materials.

Uzan (1985) proposed the modified stress-state dependent model expressed in terms of both deviator and bulk stresses, as shown below. Uzan's model can account for the shear stress effect on the resilient modulus.

$$M_r = k_1 \theta^{k_2} \sigma_d^{\ k_3} \tag{2.2}$$

where

θ = bulk stress (= $\sigma_1 + \sigma_2 + \sigma_3$),

σ_d = deviator stress (= $\sigma_1 - \sigma_3$) as defined in Figure 2.3, and

k_1, k_2, k_3 = regression constants.

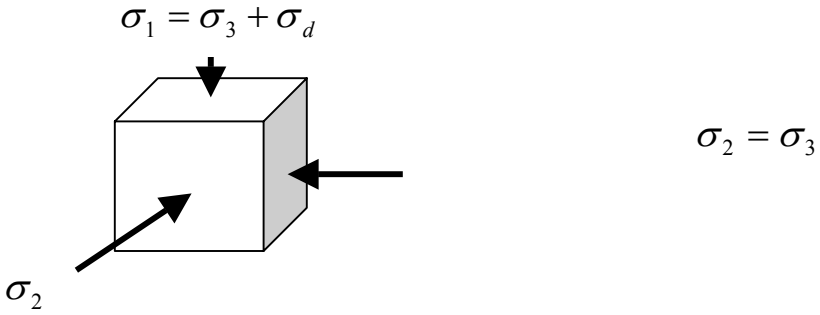

Figure 2.3 Principal stresses on a finite soil element

Elliot and David (1989) provided an improved model to represent the stress dependent behavior of granular materials above failure state. When the deviator stress exceeds the stress at failure state, the modulus of granular material tends to decrease with increasing deviator stress. The developed model is as follows:

$$M_r = \frac{k_1 \theta^{k_2}}{10^A} \tag{2.3}$$

where

$A = mR^3$,

k_1, k_2 = regression constants, and

R = stress/strength ratio.

The UT-Austin model shown below is obtained from the following procedure:

(1) measure axial strain and stress during a triaxial test,

(2) calculate moduli from the relationship between strain and stress with varying loads, and

(3) do multi regression to find coefficients (e.g., k_1, k_2, and k_3).

Finally, the model included in the parameter prediction the confining pressure and the deviator stress instead of the bulk stress (Pezo, 1993).

$$M_r = k_1 \sigma_d^{k_2} \sigma_3^{k_3} \tag{2.4}$$

where

k_1, k_2, k_3 = regression constants.

The universal model introduced by Witczak and Uzan (1988) is applicable to a wide range of unbound materials having both c and ϕ shear strength parameters. The universal model is shown as follows:

$$M_r = k_1 P_a \left(\frac{\theta}{P_a} \right)^{k_2} \left(\frac{\sigma_d}{P_a} \right)^{k_3} \tag{2.5}$$

where

P_a = atmospheric pressure,

σ_d = deviator stress (= $\sigma_1 - \sigma_3$), and

k_1, k_2, k_3 = regression coefficients.

The comparison of measured and predicted moduli of granular materials showed that the universal model improved the accuracy of prediction of resilient modulus significantly (Santha, 1994). In case of fine-grained material, it is recommended to use this model when test data has a series of confining pressure.

Tutumluer and Thompson (1997) proposed a cross-anisotropic model to predict the vertical, horizontal, and shear moduli of granular base materials. Unlike the isotropic elastic model, the nonlinear anisotropic model was able to show the variations of vertical and horizontal moduli of base materials. It is noted that the horizontal modulus is lower than the vertical modulus and the tensile stresses at the bottom of base can be reduced drastically compared to the results from isotropic elastic programs. The summary of nonlinear models for granular soils is given in Table 2.1.

2.2.2 Fine-Grained Soil

The resilient modulus of fine-grained soil is usually dependent on the deviator stress and moisture content. In general, it decreases with the increase in deviator stress (stress-softening effect). The moisture content affects the resilient modulus of fine-grained soil more significantly than that of granular material (Thadkamalla and George, 1992).

The bilinear model based on repeated axial load test shows that the resilient modulus drastically decreases as the deviator stress increases up to breakpoint, and then slightly decreases.

Table 2.1 Resilient modulus models for granular materials

Model	Model Expression	Model Constants
k - θ	$M_r = k_1\theta^{k_2}$	k_1, k_2
Uzan	$M_r = k_1\theta^{k_2}\sigma_d^{\ k_3}$	k_1, k_2, k_3
Elliot and David	$M_r = \frac{k_1\theta^{k_2}}{10^A}$	k_1, k_2, A
UT-Austin	$M_r = k_1\sigma_d^{\ k_2}\sigma_3^{\ k_3}$	k_1, k_2, k_3
Universal Model	$M_r = k_1 P_a\left(\frac{\theta}{p_a}\right)^{k_2}\left(\frac{\sigma_d}{p_a}\right)^{k_3}$	k_1, k_2, k_3, p_a

Note: M_r = resilient modulus;
θ = bulk stress = $\sigma_1 + \sigma_2 + \sigma_3$;
σ_d = deviator stress = $\sigma_1 - \sigma_3$;
σ_3 = confining stress = σ_2;
p_a = atmospheric pressure (usually 101.3 kPa or 14.7 psi)

However, Yoder and Witczak (1975) indicated that the resilient modulus increases with the deviator stress above break point. This breakpoint enables to characterize the type of subgrade soil and indicate the material response from loading condition (Thompson and Elliot, 1985).

$$M_r = k_2 + k_3(k_1 - \sigma_d) \qquad k_1 > \sigma_d$$

$$M_r = k_2 + k_4(\sigma_d - k_1) \qquad k_1 < \sigma_d \qquad (2.6)$$

As a simple model shown below, the following power model was proposed to predict stress-softening effect of a subgrade soil. Since the deviator stress decreases with depth within the subgrade, the resilient modulus varies with depth.

$$M_r = k_1 \sigma_d^{\ k_3} \tag{2.7}$$

Fredlund *et al.* (1977) studied the relationship between resilient modulus of cohesive soil and deviator stress, confining pressure, and matrix suction. Their study showed that the confining pressure made a negligible effect on the resilient modulus of cohesive soil. However, as the deviator stress and matrix suction increase, the resilient modulus of subgrade soil increase.

Table 2.2 Resilient modulus models for cohesive soils

Model	Model Expression	Model Constants
Bilinear Model	$M_r = k_2 + k_3(k_1 - \sigma_d) \quad k_1 > \sigma_d$ $M_r = k_2 + k_4(\sigma_d - k_1) \quad k_1 < \sigma_d$	k_1, k_2, k_3, k_4
Power $k - \sigma_d$	$M_r = k_1 \sigma_d^{\ k_3}$	k_1, k_3

2.3 Strain-Dependent Subgrade Model

In order to predict the strain-dependent characteristic of subgrade soil, Kim and Stokoe (1992) investigated the effect of strain amplitude and load frequency on the resilient modulus using the resonant column and torsional tests than what is typically measured in the triaxial test. Since the subgrade soil under wheel loading is subjected to lower strain levels, this approach is likely to be more realistic. The modulus obtained

from the two tests decreases with an increasing strain amplitude above 0.001 percent and independent of strain amplitude below 0.001 percent, which indicates the linear elastic behavior. In the linear behavior, the resilient modulus of a soil is independent of strain amplitude and is the maximum of modulus (E_{max}) measured. The high frequency load application tends to result in increment of subgrade modulus. They also found that the plastic index (PI) as an engineering property of soil is a good indicator in estimating resilient modulus (Figure 2.4).

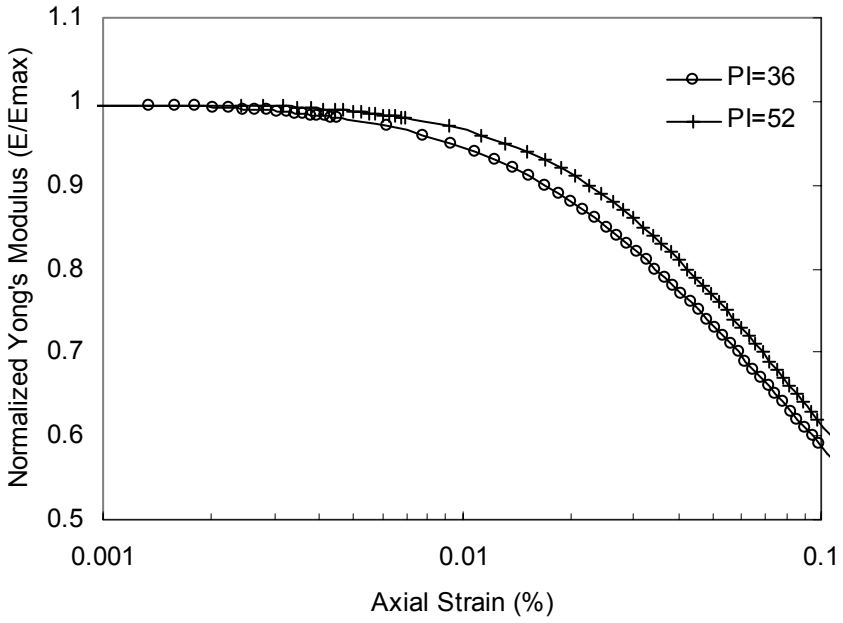

Figure 2.4 Variation in normalized Young's modulus with PI value

To fit the test data, the Ramberg-Osgood (R-O) fitting method was used as follows:

$$\varepsilon = E^{'} \cdot \varepsilon + C\left(E^{'} \cdot \varepsilon\right)^{R} \tag{2.8}$$

where

$E^{'} = E / E_{\max}$ = normalized Young's modulus and

C and R = R-O parameters.

Equation (2.8) can be rearranged:

$$\varepsilon \cdot (1 - E^{'}) = C \cdot (E^{'} \cdot \varepsilon)^{R} \tag{2.9}$$

By taking the logarithm of both sides, Equation (2.9) gives:

$$\log[\varepsilon \cdot (1 - E^{'})] = \log C + R \cdot \log(E^{'} \cdot \varepsilon) \tag{2.10}$$

Based on a least-squares method, the R-O parameter R is directly determined from the slope, and the parameter C is obtained from the intercept. This strain approach has an advantage that a single regressed model takes care of cohesive materials comparing to the stress-based models. However, the strain-based model is not accurate for granular soils because it cannot account for bulk stresses.

Borden *et al.* (1994) studied the soil response induced by vibration, which is similar to a pavement system under moving traffic loads using laboratory resonant column and torsional shear tests. They investigated the effects of soil types, confining pressure, shear strain amplitude, and number of cycles applied using resonant column and torsional shear tests. It is found that the shear modulus of the residual soils decreased and the damping ratio increased with an increasing shear strain amplitude. In addition, no significant effect of number of cycles was found on the shear modulus and damping ratio of residual soils.

CHAPTER THREE
PCC PAVEMENT ANALYSIS

The multi-layered linear elastic theory is not appropriate for the study of the behavior of subgrade under intact and rubblized PCC pavements because of its inability to account for stress-state dependence of soils. Rather, the finite element method (FEM) is the most accurate means for calculating pavement response. Finite element models are able to simulate the results of proven theories such as the multi-layered elastic theory and, further, allow the possibility of adding more complicated material models, such as stress-state dependent subgrade model, to pavement analysis.

Several finite element programs have been developed for pavement structural analyses, such as ILLI-PAVE and MICH-PAVE for flexible pavements and ILLI-SLAB for rigid pavements. The ILLI-PAVE computer program considers an axisymmetric structure for finite mesh generation and the stress-state dependent modulus for granular materials and cohesive soils. The principal stresses in granular and cohesive soils are changed at the end of iterations into a Morhr-Coulomb failure envelope if the deviator stress exceeds the failure envelope.

In this study, a commercially available finite element program, ABAQUS, was used to compute pavement responses based on dynamic analysis. Additionally, NCPAVE, recently developed by researchers at North Carolina State University, was used for static analysis with FWD multi-level loads. Issues related to the finite element modeling of PCC pavements under multi-level FWD loads are discussed in the remainder of this chapter.

3.1 FEM Program

ABAQUS has been proven suitable for pavement analysis by many researchers. Kuo *et al.* (1995) conducted a comprehensive study of various FEM pavement analysis programs and showed that the ABAQUS program yields results comparable to those of other programs. Zaghoul and White (1993) successfully employed ABAQUS for 3-D dynamic analysis of intact flexible pavements. Three-dimensional rigid pavement analyses using ABAQUS were also performed by Kuo *et al.* (1995), Mallela and George (1994), and Zaghloul *et al.* (1993). In addition, Uddin *et al.* (1995) investigated the behavior of a jointed concrete pavement under a standard FWD load with discontinuities, such as joint deterioration and transverse cracking, using ABAQUS with 3-D dynamic analysis.

ABAQUS provides many element and material models that are useful for pavement analysis. For example, the infinite element model may be used to model the infinite horizontal and vertical boundaries of a pavement profile with static, harmonic, and transient dynamic loading and thermal gradient conditions. In the case of a material model, ABAQUS is available with linear elastic, nonlinear elastic, viscoelastic, plastic, and modified elastic.

In this study, the finite element method using ABAQUS is applied to analyze pavement systems with dynamic loads, an axisymmetric structure, and a nonlinear subgrade model.

NCPAVE, a static finite element program, was developed to generate a database of deflections dependent on pavement structures and material properties. The finite element method using NCPAVE is the same as that of ABAQUS with the exception of

static analysis. In addition, NCPAVE serves as a stand-alone forward model to give surface deflections based on backcalculated subgrade characteristics and pavement structures.

3.2 Nonlinearity Using FWD Multi-Level Loads

To predict the stress-state dependence of subgrade soils under PCC slabs, a multi-level load FWD test may be used. The underlying assumption is that the stress state of subgrade after rubblization can be reproduced by applying a higher FWD load on a PCC slab prior to rubblization. The multi-level loads and backcalculated subgrade moduli allow the establishment of a stress-state dependent subgrade modulus relationship that may be used to predict the subgrade response after rubblization.

The significance of nonlinearity in the analysis of multi-load FWD deflections should be considered to determine whether multi-level loads cause enough nonlinearity in the subgrade. According to AASHTO (1993), the ratio of loads will be equal to the deflection ratio if the material is linear.

That is,

$$P_1 / P_2 = d_{1r} / d_{2r} \quad \text{or} \quad P_1 / d_{1r} = P_2 / d_{2r} \tag{3.1}$$

where

P_1 = load 1 ,

P_2 = load 2,

d_{1r} = measured deflection at a radial distance under FWD load 1, and

d_{2r} = measured deflection at a radial distance under FWD load 2.

The nonlinearity in the analysis of multi-load FWD deflection measured from intact PCC slab has been investigated using the deflection data measured from US 29. This pavement has a 14 inch thick PCC slab over cohesive soil. (Structural details of this pavement, along with the FWD test procedure, is presented later in Chaper 5.) To determine the amount of nonlinearity in the deflections, the center and seventh deflections were normalized with respect to the load level and plotted against the load level. In such a plot, the deviation from a horizontal line indicates the amount of nonlinearity in the system.

The data from five stations of US 29 have been analyzed and are plotted in Figure 3.1. It appears that nonlinear behavior is exhibited in all the stations in varying degrees. The degree of nonlinearity was calculated by dividing the difference in the normalized deflections under 9 and 15 kip loads by the deflection under the 9 kip load. The highest degree of nonlinearity was found to be around 14 % (Figure 3.2).

Based on this analysis, the multi-level loads (9, 12, and 15 kip FWD loads) cause sufficiently high stresses in subgrade under intact PCC slab. It is assumed that the deflections measured from FWD tests are appropriate to estimate the nonlinear characteristics of subgrade.

3.3 Forward Model

The development of a procedure for determining stress-state dependent properties of subgrade from multi-load deflections requires a forward model that can predict stresses in the subgrade under varying upper layer conditions. Based on the literature review in

Chapter 2 on pavement response models and nonlinear material models of subgrade, the ABAQUS finite element program was selected as the pavement response model, using Uzan's stress-state dependent model for subgrade. Dynamic analysis was performed using ABAQUS with axisymmetric finite element representation of a pavement structure. Details of the finite element analysis are described below. Figure 3.3 shows the input loading history to simulate the FWD load. A haver-sine wave form with 0.03 second duration was used.

A pavement system is modeled with an infinite boundary in the lateral direction and with semi-infinite depth for the subgrade layer. Since the area near the load is subjected to high stresses and strains compared to the boundary medium, the surface region of the model uses smaller element than those of the subgrade. This element structure is shown in Figure 3.4.

Due to the complexities involved in the analysis of deflections measured near joints or edges in PCC pavements, it is assumed that FWD tests were performed in the middle of a slab. This assumption makes axisymmetric representation of the load and pavement more realistic.

The deflections were calculated at seven sensor locations: 0, 8, 12, 18, 24, 36, and 60 inches (D_0, D_8, D_{12}, D_{24}, D_{36}, and D_{60}) from the center of load (Figure 3.5).

Figure 3.6 shows deflection time histories generated from ABAQUS dynamic analysis. The transient data are able to provide more information on the pavement condition than peak deflections only. However, due to the complexities involved in analyzing deflection time histories, peak deflections are used in this study for assessing the subgrade nonlinearity.

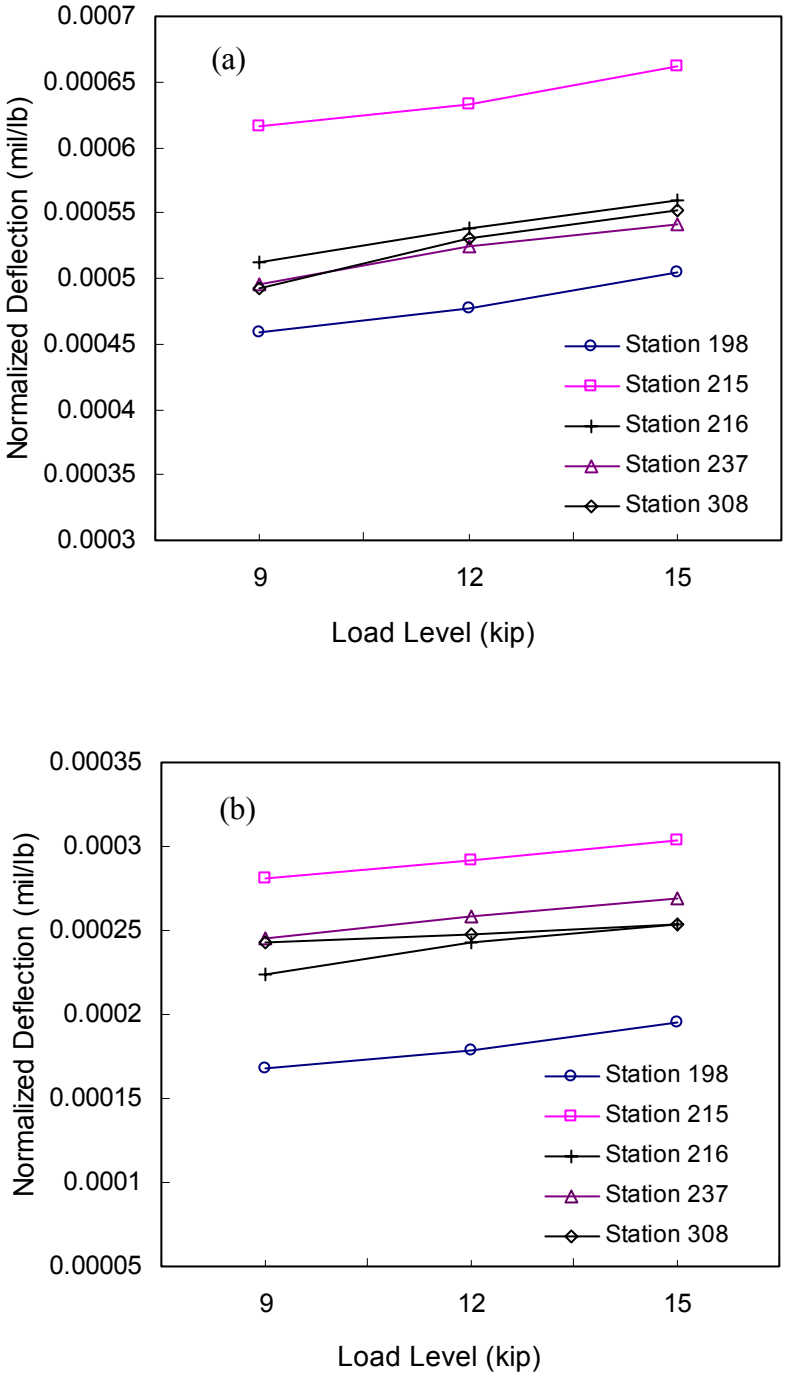

Figure 3.1 Normalized deflection vs. load level: (a) center deflection and (b) seventh deflection

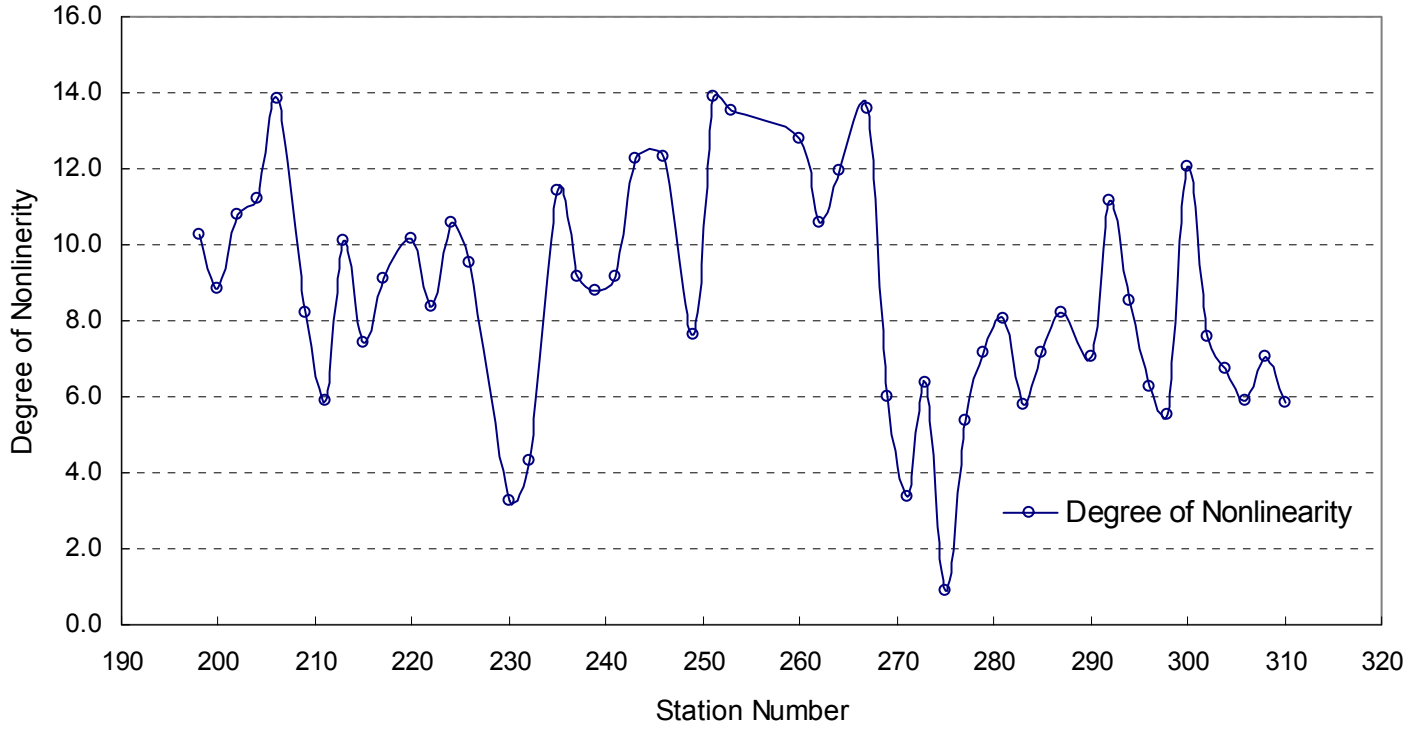

Figure 3.2 Degree of nonlinearity from US 29 FWD tests [(D_0 under 15kip – D_0 under 9kip)/D_0 under 9kip]

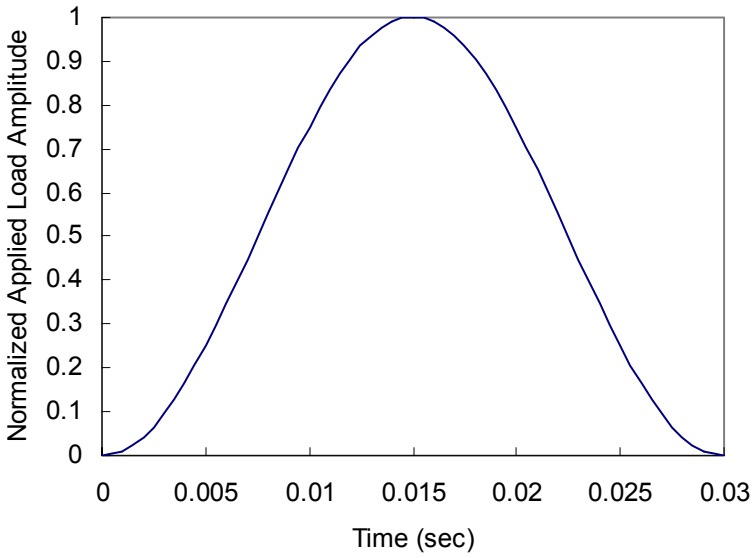

Figure 3.3 Normalized load used for dynamic analysis

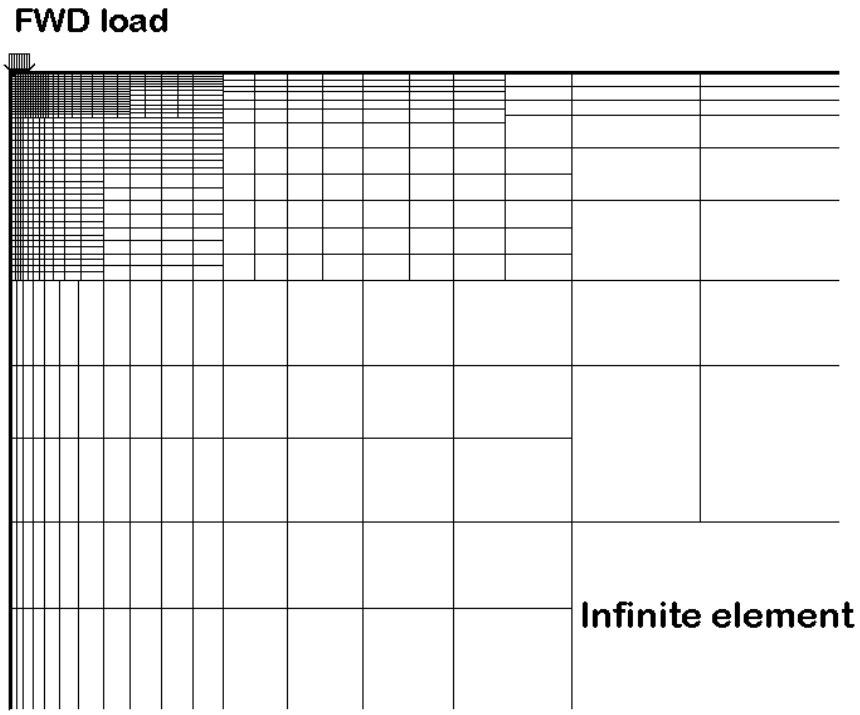

Figure 3.4 Infinite element model of a pavement system

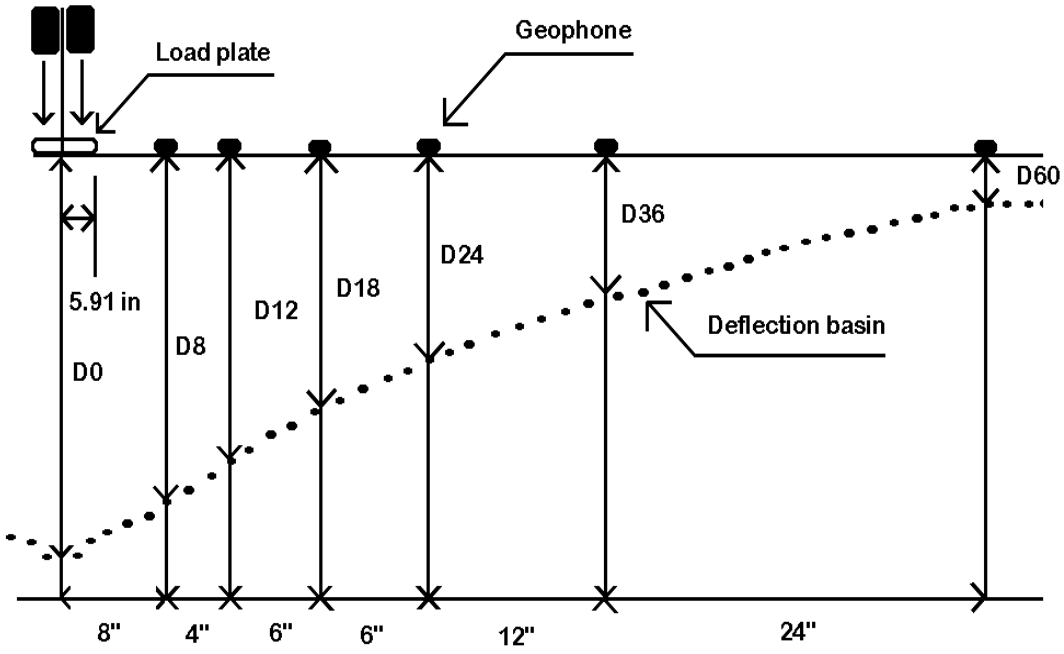

Figure 3.5 Sensor spacing and FWD testing configuration

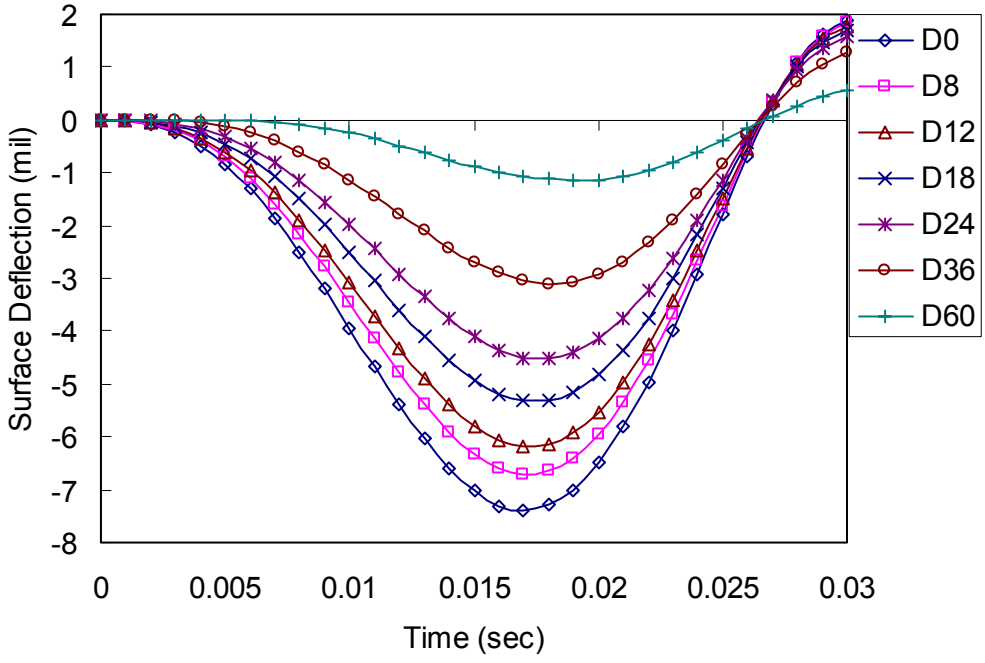

Figure 3.6 Transient deflections calculated by ABAQUS dynamic analysis

3.4 Dynamic vs. Static Analysis

Before the finite element analysis was performed on various pavement structures, a preliminary study was undertaken to investigate the significance of the difference in pavement responses between the static and dynamic analyses.

Table 3.1 summarizes the cases used in this investigation. The results are plotted in Figures 3.4 and 3.5. In this study, material coefficients from granular and cohesive soils were used to represent strong subgrades respectively.

Table 3.1 Ranges of material properties in intact PCC slab and subgrade

Layer	Thin Layer	Thick Layer	Strong Modulus	Weak Modulus
PCC Slab	6 in	16 in	5000 ksi	1000 ksi
Subgrade	5 ft	20 ft	k1=16329.96 k2=0.199 k3=-0.403 (Granular Soil)	k1=2763.60 k2=0.0 k3=-0.598 (Cohesive Soil)

This study showed that the dynamic analysis yields larger deflections than the static analysis for thin pavement structures. However, thick pavement structures exhibit different trends depending upon material properties. The following observations were made for the thick structure analysis:

1. Figure 3.8(a) shows larger outer deflections from the static analysis of a thin pavement with weak PCC and strong subgrade.
2. The case of strong PCC and strong subgrade (Figure 3.8(b)) shows larger deflections from the dynamic analysis.

3. Figures 3.8(c) and (d) (e.g., strong PCC and weak subgrade and weak PCC and weak subgrade) demonstrate that the static analysis generates larger deflections than the dynamic analysis.

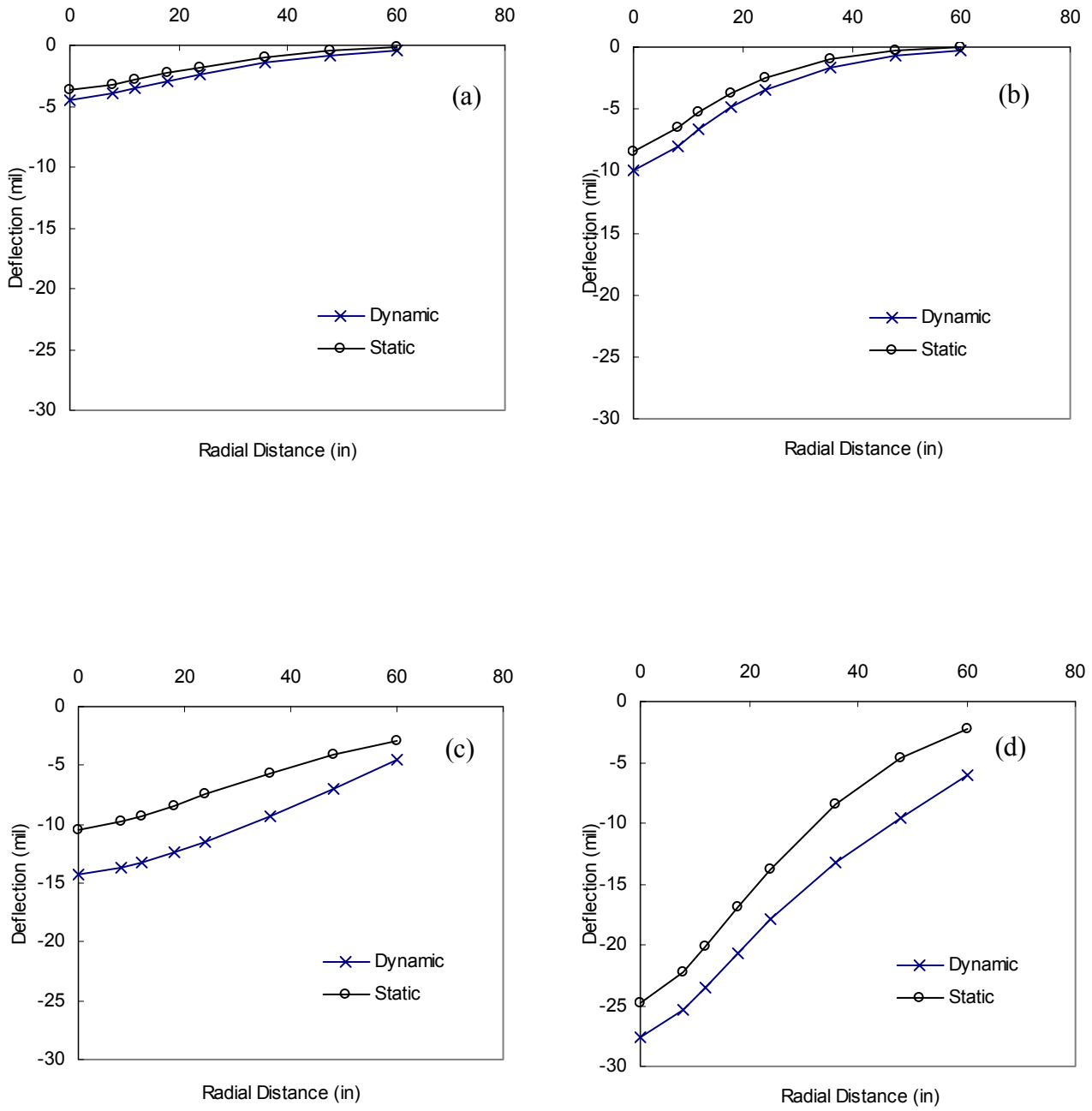

Figure 3.7 Deflection plots (a) thin structure, strong PCC and strong subgrade; (b) thin structure, weak PCC and strong subgrade; (c) thin structure, strong PCC and weak subgrade; and (d) thin structure, weak PCC and weak subgrade

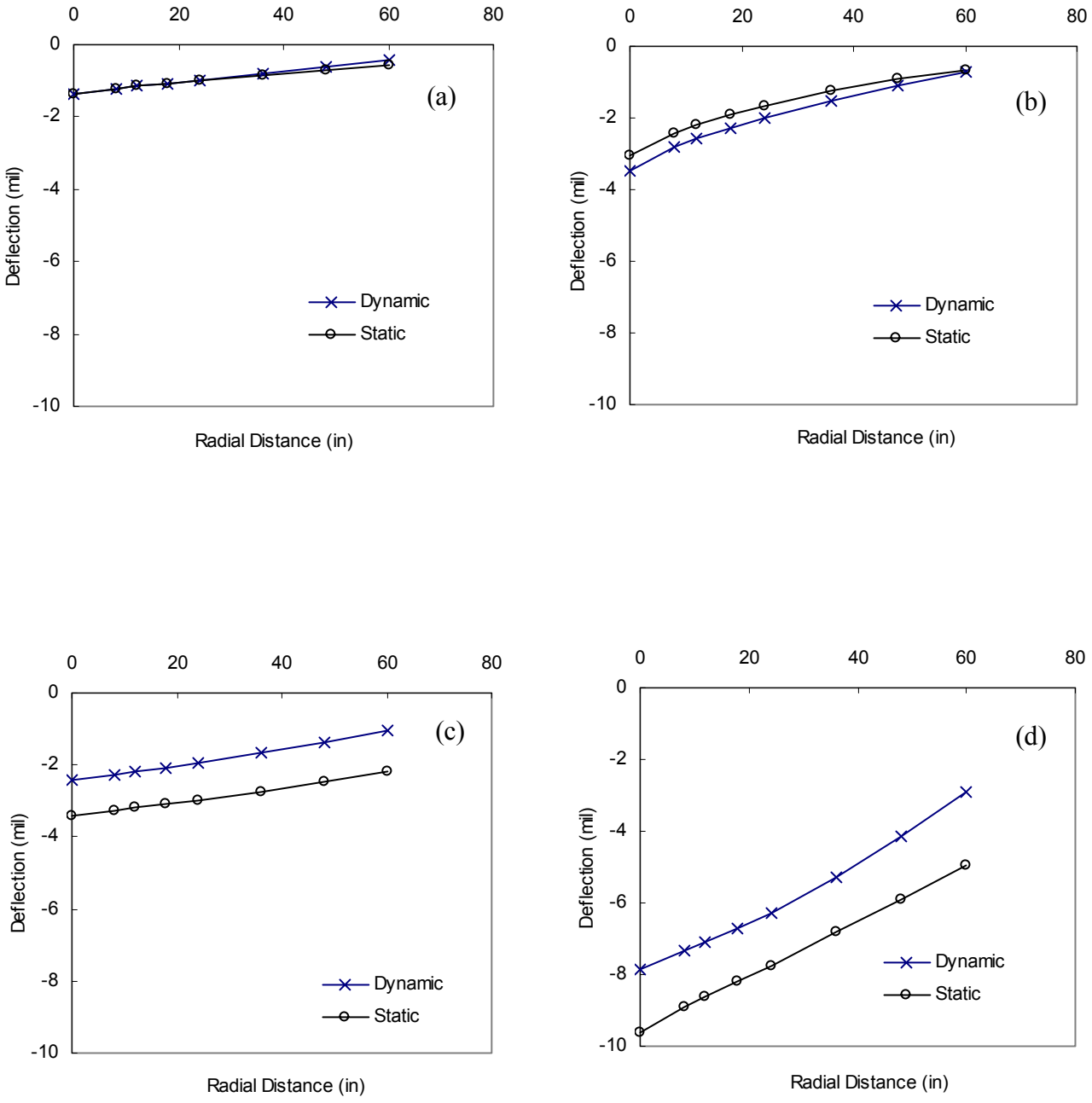

Figure 3.8 Deflection plots (a) thick structure, strong PCC and strong subgrade; (b) thick structure, weak PCC and strong subgrade; (c) thick structure, strong PCC and weak subgrade; and (d) thick structure, weak PCC and weak subgrade

CHAPTER FOUR
SUBGRADE CONDITION PREDICTION ALGORITHMS USING ANN

One of the backcalculation techniques used extensively in this research is that of artificial neural networks (ANNs). The strength of this approach (i.e., fast inversion once it is trained) is especially attractive because it counteracts the significant amount of time taken by the iterative method that is based on error minimization and that is integral to the complex forward model chosen in this research. This chapter describes the research effort that uses ANNs in different ways to predict the nonlinear characteristics of subgrade from deflections measured on PCC slabs.

In summary, ANNs were trained using the synthetic database to predict Uzan's model coefficients (k_1, k_2, and k_3) in Equation (2.2) and the strain-based model coefficients (C and R) in Equation (2.8) from multi-level load FWD deflections. ANNs were used in different ways to develop a method that would yield satisfactory performance for a set of test cases in the synthetic database. For the stress-based approach, an attempt was made to predict the nonlinear coefficients without knowing the soil type (i.e., granular versus cohesive) a priori. Poor performance from this approach suggested the need to investigate the development of an ANN-based model for cohesive soils only. Only k_1 and k_3 were predicted in this case, and improved performance resulted from this approach. The following sections describe all the efforts made in these different approaches using ANN.

4.1 Stress-Based ANN Model for General Soils

Estimation of nonlinear characteristics of subgrade using ANN requires a large database comprised of various pavement structures and layer properties. ABAQUS was run in the axisymmetric, dynamic mode with Uzan's model for subgrade to simulate the intact PCC pavement responses under multi-load FWD tests. For the static analysis, NCPAVE was run using the same structures and layer properties as in the dynamic analysis.

The input variables needed in the forward modeling include:

a) load level (9, 12, and 15 kips)

b) thickness of PCC slab (Hpcc)

c) modulus of PCC slab (Epcc)

d) thickness of subgrade (Hsg)

e) Uzan's model coefficients (k_1, k_2, and k_3)

The ranges of these input variables for forward modeling are shown in Table 4.1.

Table 4.1 The ranges of the input variables for forward modeling

Layer	Thickness			Modulus (ksi)		
	Min.	Max.	Increment	Min.	Max.	Increment
Intact PCC	6 in	16 in	1 in	500	5,000	100
Subgrade	2 ft	20 ft	1 ft	*45 cases for granular soils and 42 cases for cohesive soils		

Note : *Obtained from Lanka Santha's (1994) laboratory study of various soil's stress-state dependencies represented by Uzan's model

In Table 4.1, the maximum and minimum layer thicknesses were determined by investigating all the PCC pavement cases registered in DataPave. The PCC slab thickness

and the subgrade thickness together determine the depth to a stiff layer. The PCC slab modulus range was determined from the literature. For the subgrade modulus, a comprehensive summary of Uzan's model coefficients on various granular and cohesive soils is available in Santha (1994). These coefficients were used to represent varying soil types in pavement systems.

Random combinations of input properties were generated using the Latin hypercube random sampling technique to provide even distribution of the input properties within the ranges and the increments defined by the user. At first, a total of 2,000 cases was created for each load level. Later, 200 cases containing low moduli (500 to 900 ksi) for PCC were included to consider the case of FWD tests on distressed PCC pavements. A total of 6,600 cases (2,200 cases for each of the three load levels) was modeled for the database. Out of 6,600 cases, 6,000 randomly selected cases (2,000 cases per load level) were used to train the ANN to establish the relationship between Uzan's model coefficients and surface deflections. This relationship is represented by a network with adjusting weights and biases that yield the minimum error for prediction.

The remaining 600 cases were used for testing the trained ANN. A typical change of root-mean-square-error (RMSE) as a function of epochs (i.e., trained iterations) is shown. The optimum weights and biases in the ANN were selected when the testing RMSE was the lowest. The optimum ANN structure was determined by systematically changing the number of hidden layers and units and selecting the structure that yielded the lowest training and testing RMSEs.

If the network is trained too much, the network will learn the noise or memorize the training patterns and will not generalize well with new patterns (Kim, 1997). To prevent overtraining and in order to select an optimum structure that yields the lowest RMSE from testing, an independent testing set (100 randomly selected cases) was used as well as the training set. As shown in Figure 4.1, there is an optimum point where the testing RMSE starts to increase even though the training RMSE decreases. The network's weights at this optimum point of the lowest testing RMSE were saved.

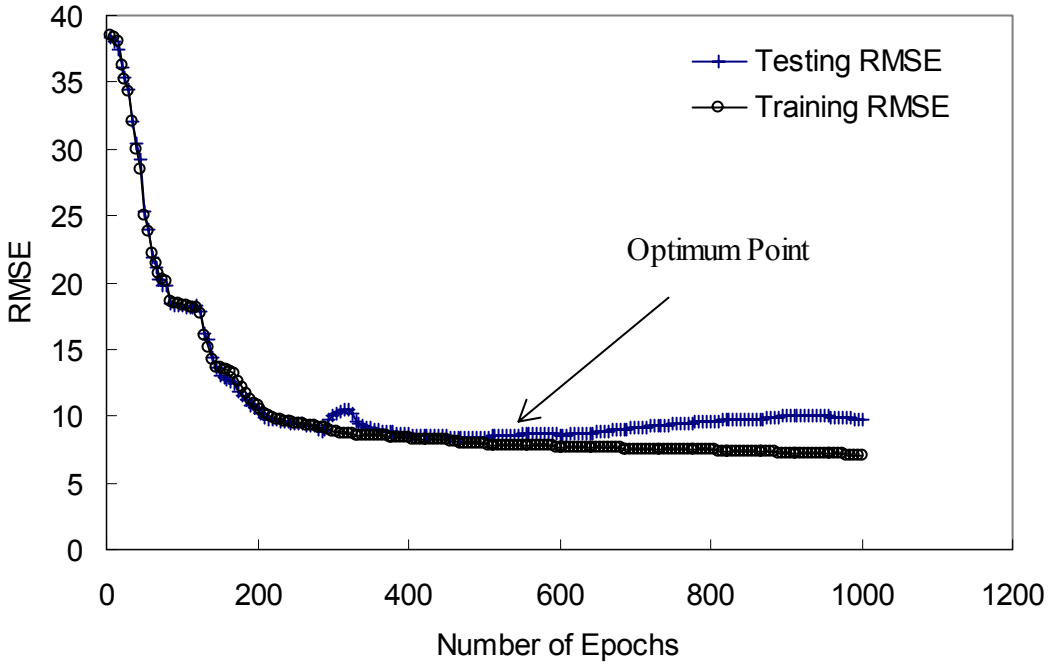

Figure 4.1 Finding optimum point using testing set

4.1.1 Direct Backcalculation

In this approach, 21 deflections generated by 3 load levels were used as inputs to directly predict k_1, k_2, and k_3. Many different hidden layer structures were tried with and without the PCC thickness as an additional input. Table 4.2 summarizes the best two structures for each of the two cases. In general, RMSEs were not satisfactory. The prediction of k_2 was much more difficult, and the inclusion of Hpcc as an additional input improved the prediction accuracy.

In order to find whether this poor prediction was due to the nature of dynamic analysis, NCPAVE was run in the static mode to develop a database that may be used to train ANNs. All other analysis features in NCPAVE were kept the same as those in ABAQUS. Using the ANNs trained by the static database, Uzan's coefficients were backcalculated and the prediction errors were compared with those from the dynamic backcalculation. It can be concluded from Table 4.3 that the static analysis does not improve the prediction accuracy compared to the dynamic analysis. This poor prediction from the direct backcalculation approach thereby required investigation into another approach which is explained in the next section.

4.1.2 Regression Approach Using ANN Backcalculated Stresses and Moduli

The regression approach is based on the observation that the prediction of pavement responses (e.g., stresses and strains) and the subgrade modulus from surface deflections is much more promising than the prediction of subgrade nonlinear properties. Once stresses and subgrade moduli are predicted, a regression analysis of them can yield

Uzan's model coefficients. The static nonlinear finite element analysis was performed on various pavement structures to compute pavement deflections and bulk and deviator in subgrade under the center of the load. Uzan's model was used for subgrade; subgrade moduli at the end of the iterations of the finite element analysis were stored in the database.

Table 4.2 Prediction RMSEs of k_1, k_2, and k_3 using dynamic database

Input	Hidden layer Structure	Output	Training Average RMSE*(%)	Testing Average RMSE (%)
D_0 to D_{60} under Multi-loads	21-25-22-1	k_1	43.60	45.55
		k_2	93.30	185.26
		k_3	3.41	12.22
D_0 to D_{60} under Multi-loads	21-26-23-1	k_1	22.35	30.0
		k_2	70.50	190.20
		k_3	4.98	11.84
D_0 to D_{60} under Multi-loads Hpcc**	22-25-22-1	k_1	10.49	35.76
		k_2	98.64	194.17
		k_3	5.58	11.23
D_0 to D_{60} under Multi-loads Hpcc	22-26-23-1	k_1	18.70	27.11
		k_2	69.35	220.0
		k_3	5.98	12.84

*RMSE : Root Mean Square Error
** Hpcc : PCC slab thickness

ANNs were trained using this database to predict subgrade moduli and bulk and deviator stresses at the top of the subgrade from surface deflections caused by 9, 12, 15 kip load levels. The accuracy of the prediction is tabulated in Tables 4.4 to 4.6. In all the cases, the testing RMSEs were below 10%, thus indicating satisfactory prediction.

Table 4.3 Prediction RMSEs of k_1, k_2, and k_3 using static database

Input	Hidden Layer	Output	Training Average RMSE (%)	Testing Average RMSE (%)
D_0 to D_{60} under Multi-loads	21-25-22-1	k_1	24.91	26.69
		k_2	166.17	251.62
		k_3	21.86	32.23
D_0 to D_{60} under Multi-loads	21-26-23-1	k_1	21.07	26.73
		k_2	192.40	265.14
		k_3	25.17	29.34

Table 4.4 Prediction accuracy of the indirect backcalculation using deflections under 9 kip FWD load

Input	Hidden layer Structure	Output	Training Average RMSE (%)	Testing Average RMSE (%)
D_0 to D_{60}	7-14-11-1	Center* Bulk Stress	1.28	1.74
	7-15-12-1		1.48	1.81
D_0 to D_{60}	7-14-11-1	Center Deviator Stress	4.35	4.66
	7-15-12-1		4.12	4.68
D_0 to D_{60}	7-14-11-1	Center Modulus	8.73	8.35
	7-15-12-1		7.86	8.86
	7-16-13-1		8.58	8.47
	7-17-14-1		8.98	8.97

*Center : The point at the top of the subgrade below the load plate of FWD

Table 4.5 Prediction accuracy of the indirect backcalculation using deflections under 12 kip FWD load

Input	Hidden layer Structure	Output	Training Average RMSE (%)	Testing Average RMSE (%)
D_0 to D_{60}	7-14-11-1	Center Bulk Stress	1.63	2.21
	7-15-12-1		1.88	2.53
D_0 to D_{60}	7-14-11-1	Center Deviator Stress	4.70	4.78
	7-15-12-1		4.86	5.49
D_0 to D_{60}	7-14-11-1	Center Modulus	8.45	9.13
	7-15-12-1		8.65	9.07
	7-16-13-1		7.83	9.52
	7-17-14-1		8.74	8.84

Table 4.6 Prediction accuracy of the indirect backcalculation using deflections under 15 kip FWD load

Input	Hidden layer Structure	Output	Training Average RMSE (%)	Testing Average RMSE (%)
D_0 to D_{60}	7-14-11-1	Center Bulk Stress	2.23	2.45
	7-15-12-1		1.72	2.59
D_0 to D_{60}	7-14-11-1	Center Deviator Stress	5.77	6.41
	7-15-12-1		4.21	5.19
D_0 to D_{60}	7-14-11-1	Center Modulus	8.49	8.70
	7-15-12-1		8.94	9.23
	7-16-13-1		8.35	9.80
	7-17-14-1		6.99	8.50

These ANNs were used to predict the subgrade modulus and bulk and deviator stresses from synthetic deflections. These predicted values were regressed to determine k_1, k_2, and k_3. They were then compared with the known values used to generate the synthetic deflections. The RMSEs were over 100% for estimating all the coefficients. The comparison was not any better than the accuracy shown in Table 4.2 from the direct backcalculation. The backcalculation procedure using the stresses under the center of the

FWD load and modulus may be sufficient to capture the nonlinearity of subgrade using the regression approach.

Based on the prediction results from the two approaches, reliable backcalculation of Uzan's model coefficients is not feasible without having more information presented to the ANN as inputs. A subgrade soil type that can be obtained by construction record or by sampling from outside shoulder areas can provide the soil type (i.e., granular versus cohesive) and may be used as an additional input. The following section describes this procedure.

4.2 Stress-Based ANN Model for Cohesive Soils

Since most of the problematic soils in pavements are categorized as cohesive soils, the research effort focused on nonlinear characterization of cohesive soils. This additional input allowed the k_2 value in Uzan's model to be set to equal zero; thus, the effect of bulk stress in cohesive soils is considered minimal.

Synthetic deflections were obtained using the ABAQUS dynamic analysis with various material properties and thicknesses. Since the laboratory resilient modulus data from I-85 soils were available at this time, these coefficients were also included in the input database. The larger thicknesses and material properties selected for the forward modeling are summarized in Table 4.7.

One thousand cases were generated randomly with these ranges. Surface deflections and deviator stresses were calculated on the pavement surface and on the subgrade at radial distances of 0, 8, 12, 18, 24, 36, and 60 inches (Figure 4.2).

Table 4.7 Material properties and thicknesses used in ABAQUS FEM

	PCC Layer	Subgrade
Modulus (ksi) or Model Constants	500 ~ 5,000 (ksi)	42 sets from Santha(1994) 3 sets from lab tests*
Thickness	2 ~ 20 ft	6 ~ 16 in

* Resilient modulus tests using cohesive soils from I-85

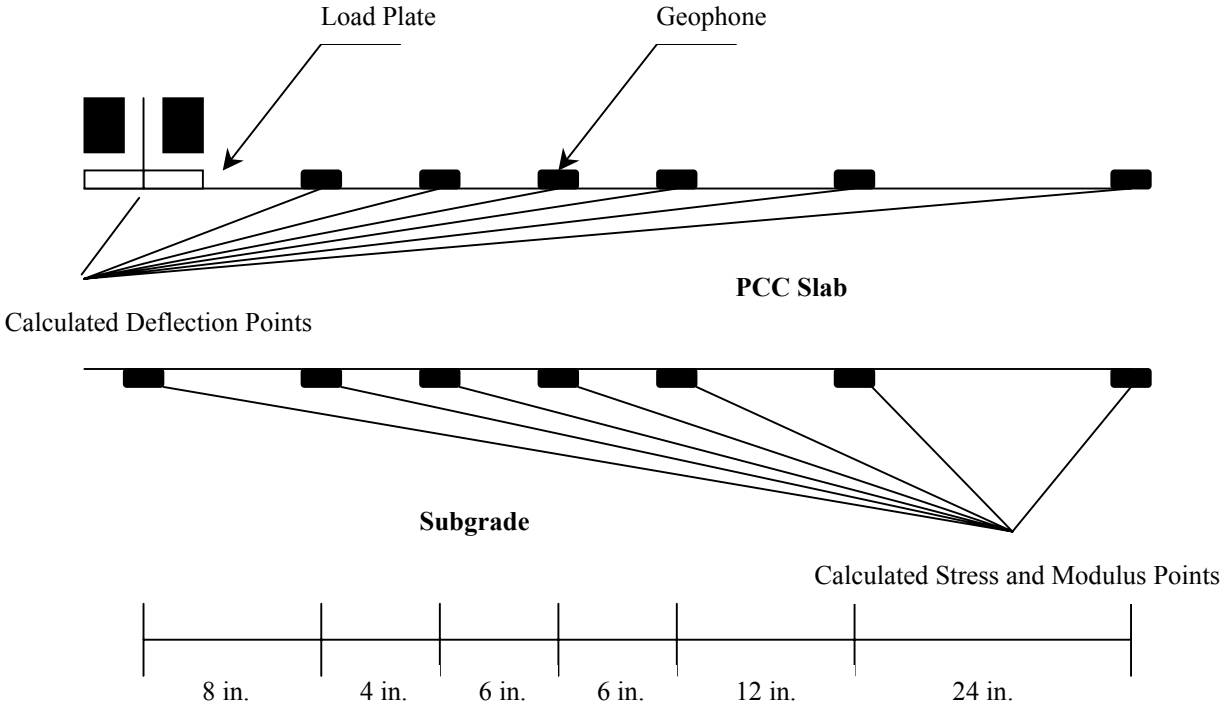

Figure 4.2 Locations of calculated deflections, deviator stresses, and moduli

The same two approaches (direct and regression) made in the general soil case were applied to the cohesive soil case to backcalculate the nonlinear coefficients. The results are presented in the following sections.

4.2.1 Direct Backcalculation for Cohesive Soils

The RMSEs of the training and testing cases are shown in Table 4.8 as a function of input types and the network structure used to backcalculate the coefficients.

Table 4.8 Prediction accuracy of the direct backcalculation using different input units under multi FWD loads

Input		Hidden layer Structure	Output	Training Average RMSE (%)	Testing Average RMSE (%)
ANN_1	D_{24}, D_{36}, D_{60}, Hpcc	11-8-1	k_1	12.07	11.08
		12-9-1		**9.17**	**10.29**
		13-10-1		10.52	11.88
		11-8-1	k_3	**12.90**	**10.09**
		12-9-1		18.09	11.34
		13-10-1		19.82	12.71
ANN_2	D_0 to D_{60}, Hpcc	11-8-1	k_1	6.70	8.96
		12-9-1		**10.12**	**7.64**
		13-10-1		8.45	7.85
		11-8-1	k_3	**11.92**	**9.96**
		12-9-1		16.69	10.94
		13-10-1		14.62	9.97
ANN_3	AREA, D_{24}, D_{36}, D_{60}, Hpcc	11-8-1	k_1	9.77	8.26
		12-9-1		**5.55**	**7.16**
		13-10-1		4.58	8.00
		11-8-1	k_3	**9.43**	**9.32**
		12-9-1		7.78	10.14
		13-10-1		9.89	10.95
ANN_4	BDI, F2, D_{24}, D_{36}, D_{60}, Hpcc	11-8-1	k_1	5.01	8.17
		12-9-1		**6.61**	**7.29**
		13-10-1		13.80	9.16
		11-8-1	k_3	**7.82**	**7.63**
		12-9-1		8.22	8.47
		13-10-1		11.21	7.92

From the results of the direct backcalculating procedure, the prediction accuracy is less than that of previous approaches. The optimum networks (the structures boldly marked in Table 4.8) for different input types are evaluated using field FWD data in Chapter 5.

4.2.2 Regression Approach for Cohesive Soils

Deviator stresses and moduli at the seven locations on the top of the subgrade (Figure 4.2) were backcalculated from the multi-load FWD deflections. The network sizes and the accuracy of the prediction are presented in Tables 4.9 and 4.10. These stresses and moduli were regressed to determine k_1 and k_3 in Uzan's model. Figure 4.3 shows typical relationships between the predicted moduli and deviator stresses in a logarithmic scale.

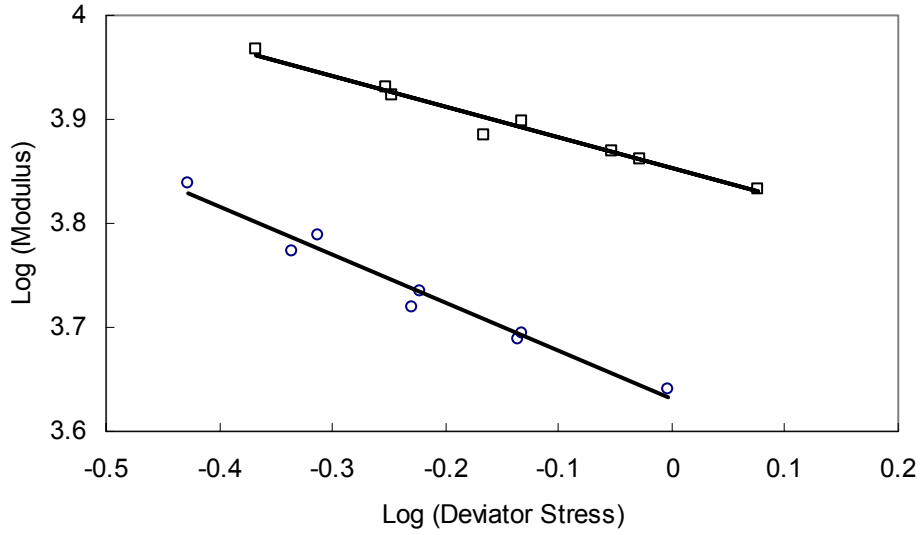

Figure 4.3 Two examples of the regression approach

In Tables 4.9 and 4.10, stresses at only four locations (0, 8, 12, and 18 inches from the load center) are presented as output. A closer examination of the stress distribution in the seven locations revealed that stresses at a radial distance greater than 18 inches were too low to cause nonlinearities in the subgrade. Therefore, it was decided to use the deviator stresses and moduli at the first four locations (0, 8, 12, and 18 inches from the load center) in the regression approach.

Table 4.9 Prediction RMSEs of deviator stresses on top of subgrade using the calculated D_0 to D_{60} deflections based on ABAQUS dynamic FEM

Input	Hidden Layer	Output	Training Average RMSE (%)	Testing Average RMSE (%)
D_0 to D_{60} under 9 kip FWD Load	7 - 4 - 1	Stress* below D_0	7.64	6.07
		Stress below D_8	6.10	6.16
		Stress below D_{12}	5.20	5.11
		Stress below D_{18}	4.42	4.15
D_0 to D_{60} under 12 kip FWD Load	7 - 4 - 1	Stress below D_0	8.41	8.00
		Stress below D_8	8.24	7.51
		Stress below D_{12}	5.47	5.49
		Stress below D_{18}	4.24	4.04
D_0 to D_{60} under 15 kip FWD Load	7 - 4 - 1	Stress below D_0	8.47	8.99
		Stress below D_8	6.85	6.83
		Stress below D_{12}	5.75	5.84
		Stress below D_{18}	4.51	4.48

* Stress is deviator stress

This approach was applied to all the synthetic data to predict the k_1 and k_3 values. These predicted values were compared with the values used as input to generate the synthetic deflections. The RMSEs from this comparison are shown in Table 4.11. The prediction accuracy of the coefficient k_1 may be within acceptable error ranges, but that of k_3 is not.

Table 4.10 Prediction RMSEs of moduli on top of subgrade using the calculated D_0 to D_{60} deflections based on ABAQUS dynamic FEM

Input	Hidden Layer	Output	Training Average RMSE (%)	Testing Average RMSE (%)
D_0 to D_{60} under 9 kip FWD Load	7 - 4 - 1	Modulus below D_0	10.07	7.07
		Modulus below D_8	9.36	7.48
		Modulus below D_{12}	9.14	7.14
		Modulus below D_{18}	11.89	7.69
D_0 to D_{60} under 12 kip FWD Load	7 - 4 - 1	Modulus below D_0	10.95	8.62
		Modulus below D_8	11.95	8.29
		Modulus below D_{12}	10.48	8.83
		Modulus below D_{18}	10.22	8.36
D_0 to D_{60} under 15 kip FWD Load	7 - 4 - 1	Modulus below D_0	12.57	10.23
		Modulus below D_8	11.00	8.14
		Modulus below D_{12}	9.59	7.72
		Modulus below D_{18}	10.46	8.40

Table 4.11 Prediction accuracy of the regression approach

	RMSE of k_1 (%)	RMSE of k_3 (%)
Training Case	18.39	60.67
Testing Case	17.12	56.51

Table 4.12 Prediction RMSEs of stresses on top of subgrade using the calculated D_0 to D_{24} deflections based on ABAQUS dynamic FEM

Input	Hidden Layer	Output	Training Average RMSE (%)	Testing Average RMSE (%)
D_0 to D_{24} under 9 kip FWD Load	10 – 7 - 1	Stress below D_0	11.47	14.57
		Stress below D_8	8.56	10.60
		Stress below D_{12}	7.96	9.01
		Stress below D_{18}	6.77	7.77
D_0 to D_{24} under 12 kip FWD Load	10 – 7 - 1	Stress below D_0	10.95	12.19
		Stress below D_8	8.67	9.84
		Stress below D_{12}	8.81	9.06
		Stress below D_{18}	6.59	7.94
D_0 to D_{24} under 15 kip FWD Load	10 – 7 - 1	Stress below D_0	11.89	11.82
		Stress below D_8	9.89	10.82
		Stress below D_{12}	8.02	9.00
		Stress below D_{18}	6.87	7.44

Based on the results in Tables 4.12 to 4.14, it was concluded that the regression approach yields a reasonable prediction of k_1 and relatively poor prediction of k_3. Figure 4.4 presents the actual and predicted values of the nonlinear coefficients that resulted from stresses and moduli estimated from the 10-7-1 structure (k_1 prediction) and the 15-13-1 structure (k_3 prediction), respectively, for 900 randomly selected cases.

Table 4.13 Prediction RMSEs of moduli on top of subgrade using the calculated D_0 to D_{24} deflections based on ABAQUS dynamic FEM

Input	Hidden Layer	Output	Training Average RMSE (%)	Testing Average RMSE (%)
D_0 to D_{24} under 9 kip FWD Load	13 - 10 - 1	Modulus below D_0	9.63	12.68
		Modulus below D_8	10.26	11.04
		Modulus below D_{12}	10.90	10.92
		Modulus below D_{18}	8.51	11.35
	15 – 13 - 1	Modulus below D_0	12.61	11.92
		Modulus below D_8	11.22	11.07
		Modulus below D_{12}	11.78	11.20
		Modulus below D_{18}	10.79	11.93
D_0 to D_{24} under 12 kip FWD Load	13 - 10 - 1	Modulus below D_0	13.49	12.46
		Modulus below D_8	13.36	12.15
		Modulus below D_{12}	9.34	12.95
		Modulus below D_{18}	9.52	11.93
	15 – 13 - 1	Modulus below D_0	14.18	13.03
		Modulus below D_8	12.16	12.10
		Modulus below D_{12}	11.43	11.33
		Modulus below D_{18}	12.21	11.71
D_0 to D_{24} under 15 kip FWD Load	13 - 10 - 1	Modulus below D_0	15.25	13.89
		Modulus below D_8	14.26	12.32
		Modulus below D_{12}	13.65	12.13
		Modulus below D_{18}	15.63	12.11
	15 – 13 - 1	Modulus below D_0	12.86	12.46
		Modulus below D_8	13.06	11.45
		Modulus below D_{12}	13.12	12.09
		Modulus below D_{18}	13.31	12.36

Table 4.14 Prediction accuracy using the calculated D_0 to D_{24} deflections according to ANN structure

Hidden Layer of ANN		Case	RMSE of k_1 (%)	RMSE of k_3 (%)
Stress Prediction	Modulus Prediction			
10 – 7 – 1	13 – 10 – 1	Training Set	17.95	56.88
		Testing Set	16.05	69.24
10 – 7 – 1	15 – 13 - 1	Training Set	16.83	50.52
		Testing Set	15.80	57.27

4.3 Strain-Based ANN Model for Cohesive Soils

Based on strain-dependent characteristics of soils, a forward model using ABAQUS was developed to simulate the strain responses influenced by FWD multi-level loads. This FEM model was implemented based on a static analysis with an incremental load similar to a dynamic load. The incremental load allowed strains to converge into a specific tolerance with an iterative method. In general, each modulus during the iteration is changed according to the state of strain. Finally, the converged moduli on top of the subgrade are calculated with the strains.

Input variables needed in the forward modeling are the same as those from the stress-state dependent model except that Uzan's model coefficients are replaced with the $E/E_{\max}$ vs. strain characteristic curve of soils. The ranges of these input variables are shown in Table 4.15.

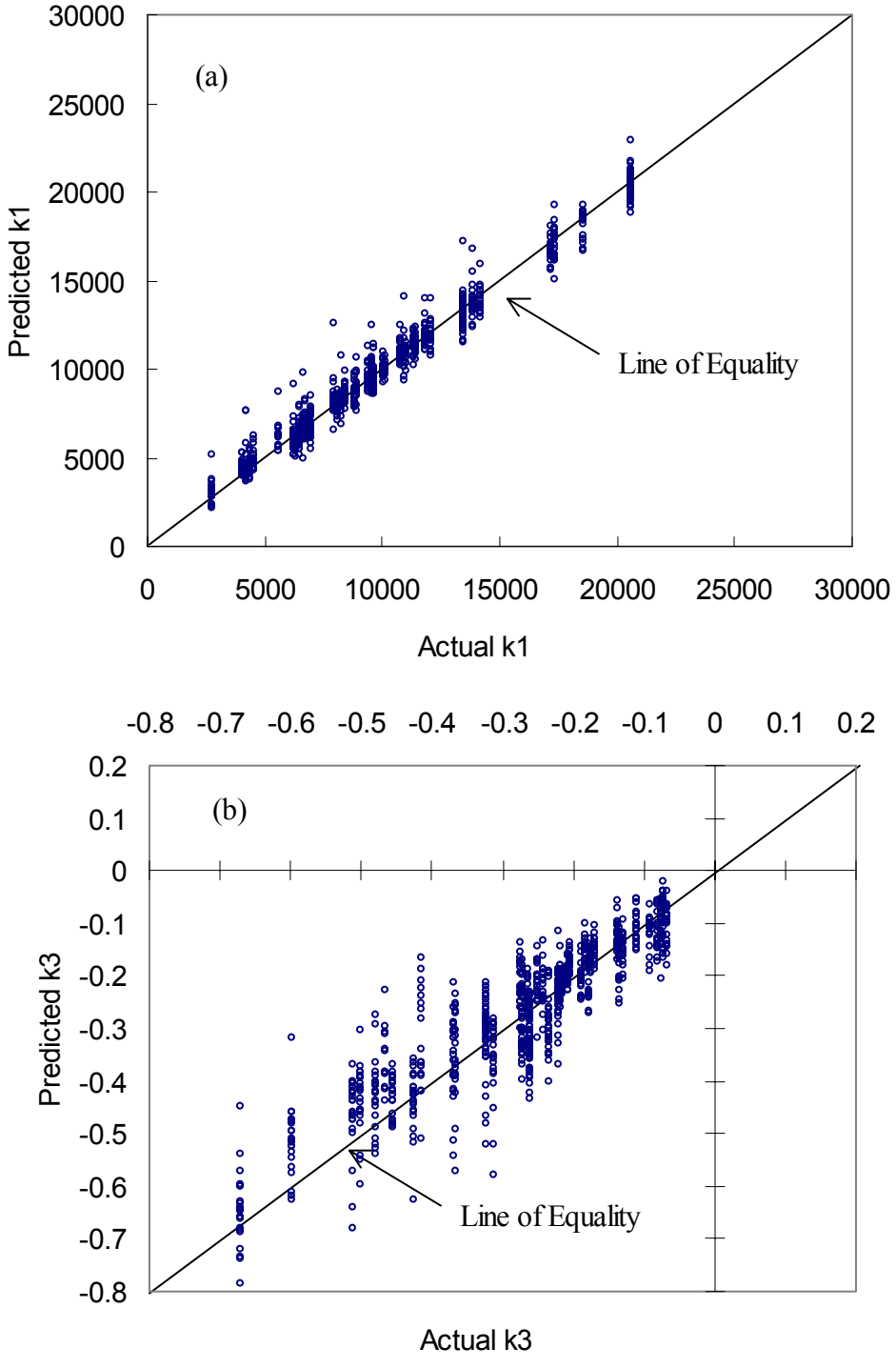

Figure 4.4 Prediction of Uzan's coefficients (a) k_1 and (b) k_3

Table 4.15 Ranges of the input variables to be used in forward modeling for the strain-based approach

Layer	Thickness	Modulus (ksi)
	Randomized Selection within Ranges	
Intact PCC	6 ~ 16 in	500 ~ 5,000 ksi
Subgrade	2 ~ 20 ft	*5 cases for subgrade soils

Note : *Obtained from Kim's (1992) on laboratory study of various soil's strain-state dependencies.

4.3.1 Backcalculation Using ANN

A total of 3,000 cases (1,000 cases for each of the three load levels) was generated for the input values of the strain-based forward model. The network sizes and the information of the training and testing cases are shown in Table 4.16. The errors between actual values (radial moduli and strains at the top of subgrade under multi-level loads) and predicted values are small (less than 7 % RMSE). However, the calculated coefficients, R and C shown in Equation 4.1 obtained from the relationship between backcalculated moduli and strains using the ANN, did not match the input coefficients for the strain-based forward model resulting in over 500 % RMSE.

$$\log[\varepsilon \cdot (1 - E^{'})] = \log C + R \cdot \log(E^{'} \cdot \varepsilon) \tag{4.1}$$

where

ε : strain, and

$E^{'}$: $E / E_{\max}$.

In order to handle this problem, the normalized modulus versus strain reduction curves (Figure 4.5) were observed to determine whether a single unique curve could represent subgrade soils with varying $E_{\max}$. The selected unique curve was compared to

two lines having minimum and maximum PI values respectively, and the error was less than 20 %. From this observation, it was found that subgrade soils tend to depend upon $E_{\max}$.

The relationship between the normalized Young's modulus and axial strain was found to be valid for North Carolina soils (Borden *et al.*, 1994). Figure 4.6 shows the selected curve and data obtained from the NC soils. The selected curve is positioned somewhat higher than the average curve, but well within the data range. Finally, the ANN's prediction of $E_{\max}$ was performed using deflections (D_0 to D_{24}) under a 9 kip FWD load, and the backcalculating RMSE was less than 5 %.

Table 4.16 Prediction RMSEs of strains and moduli at the top of subgrade using the calculated D_0 to D_{24} deflections

Input	Hidden Layer	Output	Training Average RMSE (%)	Testing Average RMSE (%)
D_0 to D_{24} under 9 kip FWD Load	12-9-1	Modulus below D_0	5.82	4.97
		Modulus below D_8	5.49	4.40
		Modulus below D_{12}	5.55	3.77
		Modulus below D_{18}	5.92	3.63
	12-9-1	Strain below D_0	2.51	1.85
		Strain below D_8	2.40	1.66
		Strain below D_{12}	2.56	1.67
		Strain below D_{18}	2.70	1.55
D_0 to D_{24} under 12 kip FWD Load	12-9-1	Modulus below D_0	5.95	5.80
		Modulus below D_8	6.38	4.50
		Modulus below D_{12}	5.14	4.68
		Modulus below D_{18}	4.98	4.69
	12-9-1	Strain below D_0	2.72	2.06
		Strain below D_8	2.74	2.05
		Strain below D_{12}	2.14	1.77
		Strain below D_{18}	2.85	1.95

The reason for using a single load, 9 kips, is that $E_{\max}$ can be caused under small loads. The model evaluation using field deflections is discussed in Chapter 5.

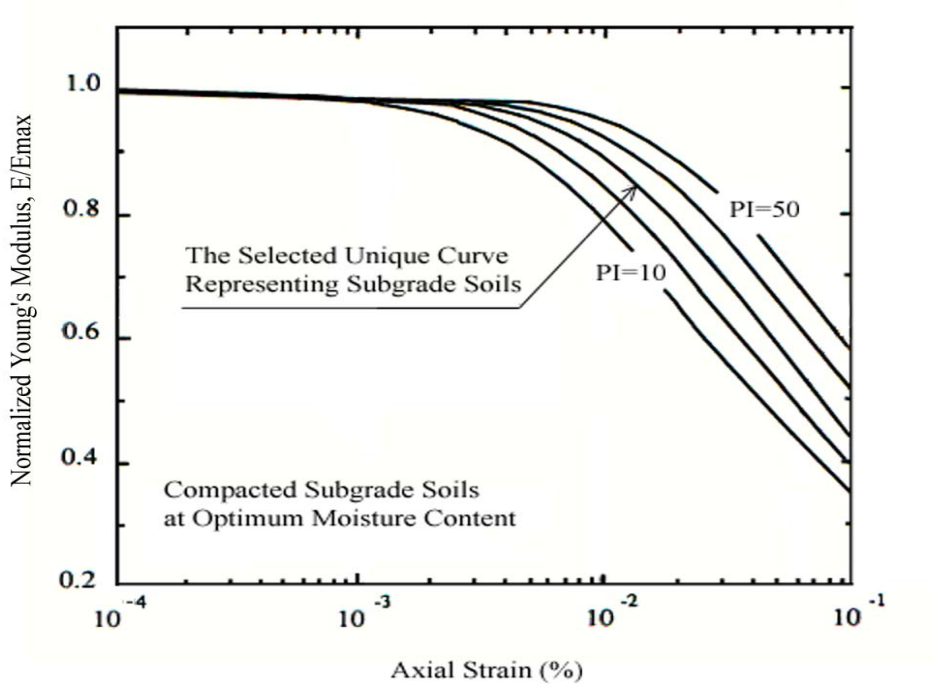

Figure 4.5 Variation in normalized Young's modulus vs. axial strain (From Kim, 1992)

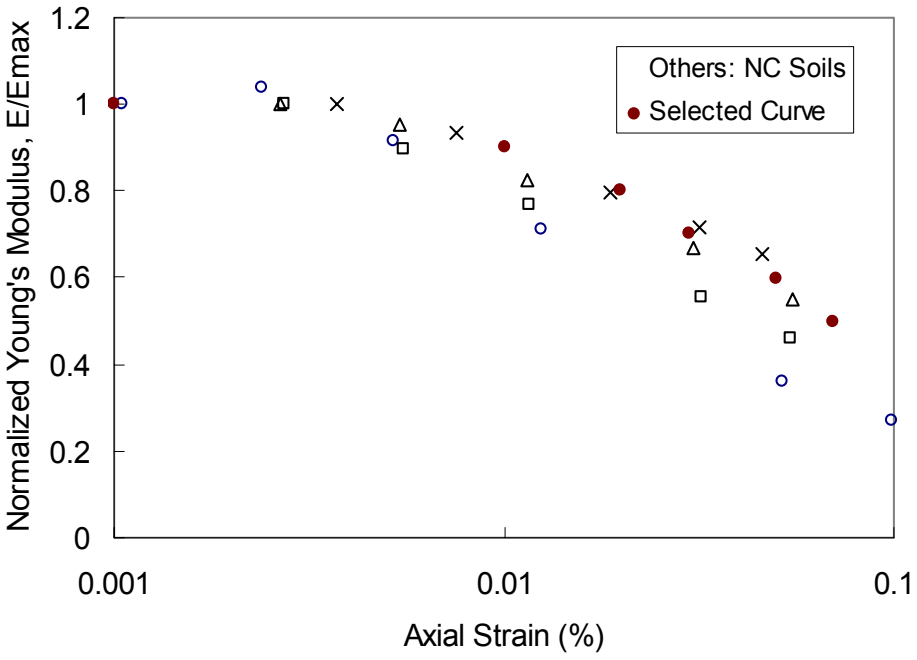

Figure 4.6 Comparison between selected curve and curves obtained from lab tests using NC soils.

CHAPTER FIVE
PERFORMACE EVALUATION OF DEVELOPED PROCEDURES

5.1 In -Situ FWD Database

The subgrade condition prediction algorithm presented in Chapter 4 requires verification using deflections and subgrade condition data obtained from actual pavements. Since the developed methods require deflections under multi-level FWD loads as input, most of the existing data obtained under a 9 kip load are not useful. During the project period, two projects were identified for this purpose by the Pavement Management Unit of the North Carolina Department of Transportation. Multi-load FWD tests were conducted on PCC slabs and on the sublayer after PCC slabs were removed. Information on these pavements is given in Table 5.1, and detailed test procedures are presented in the following sections.

Table 5.1 Layer information and locations in the tested pavement

Project ID	US 29	I-85
County	Guilford	Rowan
H_{pcc}[a]	Approx. 14 in.	9 to 10 in.
H_{base}[b]	None	5 in.
Subgrade Type	Cohesive	Cohesive
DSL[c]	Unknown	Infinite

Note : [a] PCC thickness [b]Base layer thickness
[c]Depth to a stiff layer

5.1.1 Highway US 29

FWD tests were carried out on the north bound lane of US 29 near Greensboro on August 17, 2000 for the pre-rubblization evaluation, August 19th for the post-

rubblization evaluation, and September 7th for the post-overlay evaluation. FWD deflection data were collected from a total of 51 locations beginning at station 198 with a 200 ft spacing between the test locations. FWD tests on intact PCC slabs were conducted using three different loads (9,000, 12,000 and 15,000 lbs) at the center of the slabs that were in a relatively good condition. The thicknesses of the PCC slab and AC overlay were about 14 and 8 inches, respectively.

The FWD deflection profiles along the entire US 29 project are presented in Figure 5.1. During the rubblization, an undercut was made at station 216 and between stations 254 to 259 because of poor subgrade. Since the undercut between stations 254 to 259 had already been made on both the north and southbound lanes when the southbound lane was rubblized, the pre-rubblization FWD data from these locations were not available. At station 216 only one set of multi-level load FWD deflections was collected. However, the deflection data from station 216 showed an irregular deflection bowl under the 9,000 lb load as shown in Figure 5.2. These problems on the locations with weak subgrade were critical in the analysis scheme employed in this research and therefore limit the use of the US 29 data for verification.

5.1.2 Interstate Highway I-85

Multi-level load FWD tests were conducted on the north bound lane of the exit ramp to Peeler Road from I-85 on April 14, 2000. First, FWD tests were performed at seven locations on PCC slabs using four different loads (3, 6, 9, and 12 kips). The PCC slabs were then carefully removed so as not to disturb the layer beneath them. FWD tests were conducted at 4 locations on the bare base using 3, 5, 7, and 9 kip FWD loads,

followed by Dynamic Cone Penetrometer (DCP) tests on these locations to determine the condition of the base and subgrade layers. Also, soil samples were obtained using a Shelby tube from five of the seven FWD testing locations. These samples were transported to the NCDOT Geotechnical Unit for determination of soil types and resilient moduli. Two locations were bored down to 15 ft below the pavement surface to determine the presence of a stiff layer. No stiff layer was found from the boring.

It must be noted that there were intermittent heavy rainfalls during the FWD and DCP tests. It is reasonable to assume that the FWD deflections after the slab removal, soil samples, and possibly the DCP data would be affected somewhat by these rainfalls. Another problem with the deflection data is that the highest FWD load on the PCC slab was 12 kip, not 15 kip due to the limitation in the FWD. Also, 3 and 6 kip loads on PCC slabs would not produce sufficiently high stress states to cause nonlinearity in subgrade behavior. These shortcomings left only two load levels applicable to pre-rubblization deflection analysis for determination of subgrade nonlinearity.

The I-85 data are different from the US 29 data in that the project length is fairly short and thus the subgrade stiffness may not vary significantly. However, the major advantage is that a relatively complete data set is available from the project (i.e., deflection data from PCC slabs and bare base, DCP data, and laboratory resilient modulus data). The verification study in remaining part of this chapter will therefore on the use of I-85 data.

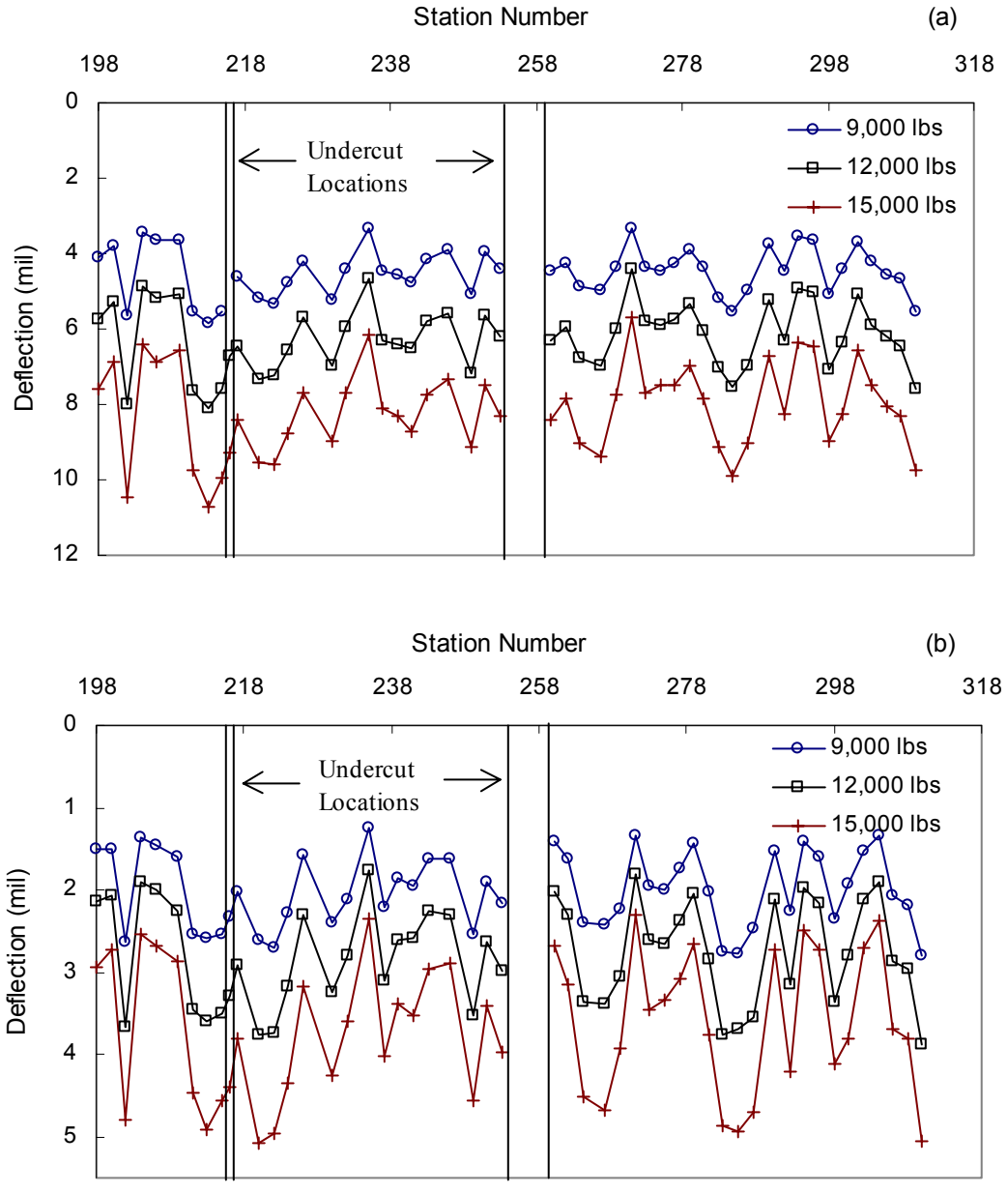

Figure 5.1 Deflection profiles for US 29 before rubblization: (a) D_0 and (b) D_{60}

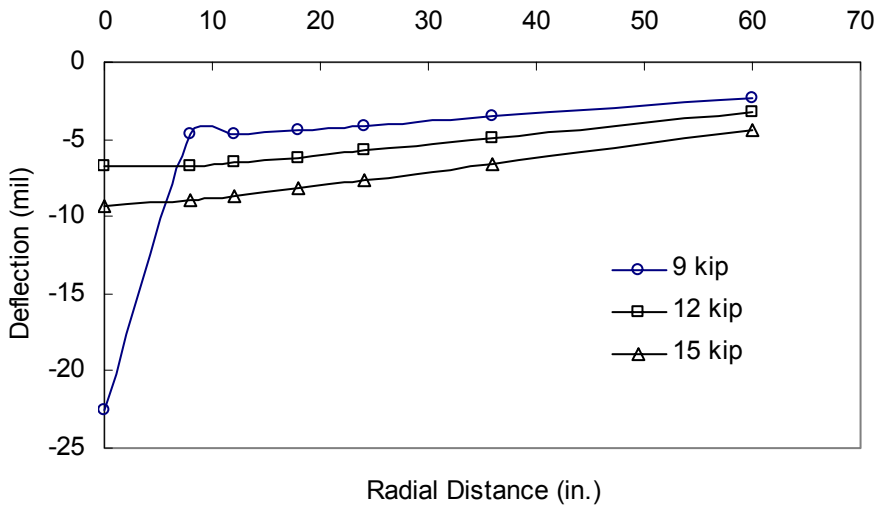

Figure 5.2 FWD deflections at station 216 on US 29

5.2 Deflection Basin Parameter Approach

Findings from a previous NCDOT research project (Kim *et al.*, 1997) show that the relationship between BDI and F2 is uniquely defined for each value of a subgrade modulus. The strength of this relationship is that it is not affected by the upper layer condition. Therefore, even though this relationship was verified only for flexible pavements, it was tried on the data from US 29.

BDI and F2 were calculated using the 9, 12, and 15 kip deflection data and plotted in Figure 5.3. It can be seen that the data point representing the undercut area (station 216) is positioned lower than most of the data points, indicating that the estimated subgrade modulus from the undercut location would be lower than that from other locations. However, there are several locations that have lower moduli than the undercut location and did not require undercutting during the rubblization. This observation suggests that the subgrade modulus backcalculated from the BDI-F2 relationship may not

be a reliable indicator for the strength of subgrade under intact PCC slabs, although this observation is based on the fairly limited data from US 29.

5.3 Prediction of Subgrade Nonlinearity Using Field FWD Deflections

The procedures presented in Chapter 4 were evaluated using the synthetic data, but the ultimate test is how well these procedures work for the field data. Unfortunately, limited field data were available for this task. The most complete field data set was obtained from the I-85 investigation.

The I-85 database includes: (1) multi-load deflections on PCC slabs; (2) multi-load deflections on a bare base after PCC slabs were removed; and (3) laboratory resilient modulus data at different stress states from soil samples collected after the FWD tests. With this data set, nonlinear characteristics of subgrade soils under PCC slabs may be predicted using the procedures presented in Chapter 4 and may be used in forward modeling to predict the multi-load deflections on bare base. Also, these nonlinear coefficients may be compared against values determined from the laboratory resilient modulus test. The procedure that yields the best match will be selected for recommendation.

The major shortcomings of the I-85 data are that only 9 and 12 kip deflections are available from the PCC slab testing and, secondly, that intermittent rains between PCC slab testing and bare base testing may have an effect on bare base deflections and soil samples obtained from the site. The lack of the 15 kip deflections will undoubtedly affect the performance of the developed procedures because, simply, three points are necessary to construct a nonlinear curve.

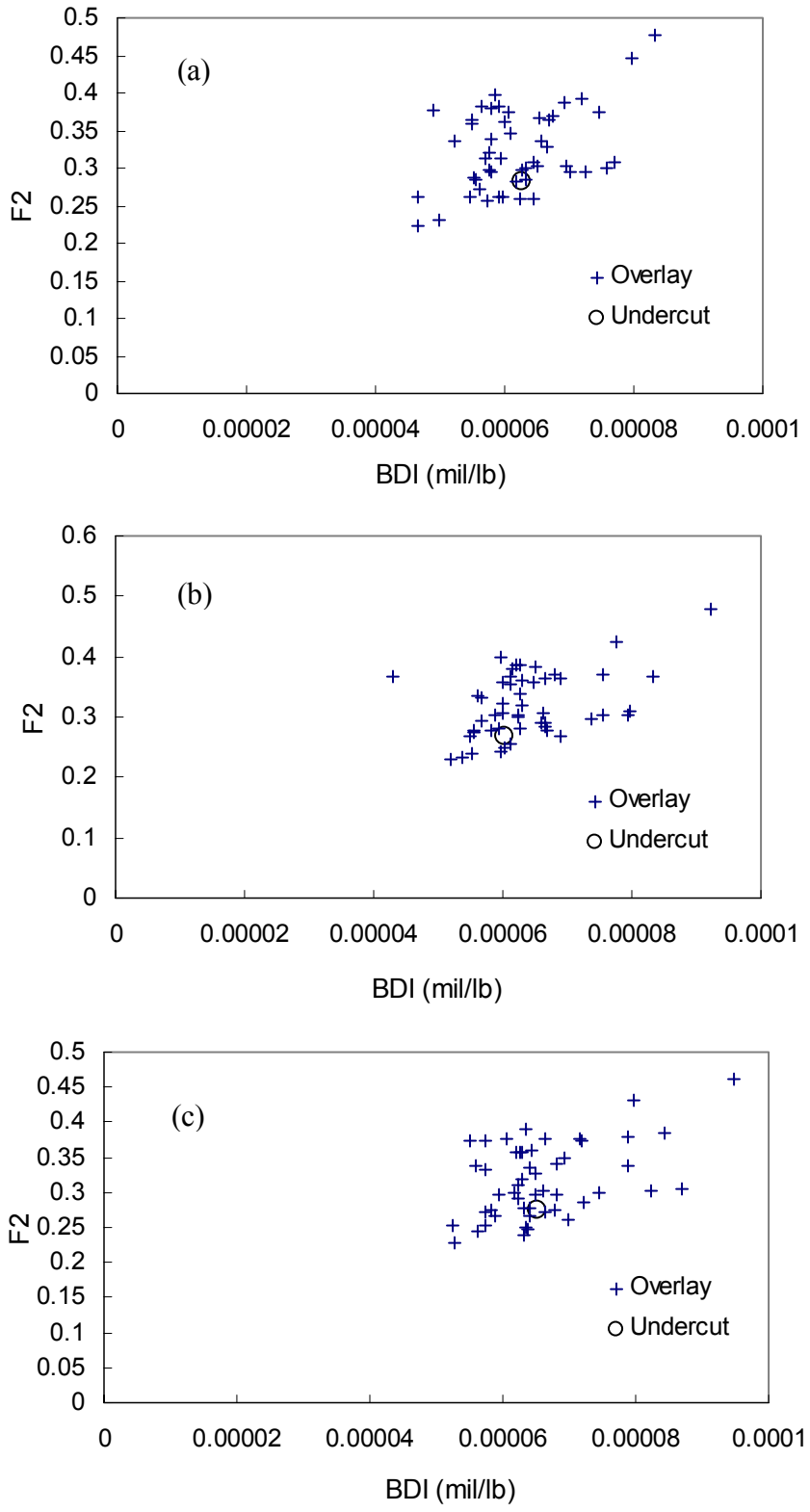

Figure 5.3 BDI vs. F2: (a) under 9 kips; (b) under 12 kips; and (c) under 15 kips

Four different approaches were tested using the field data: (1) direct prediction of the nonlinear coefficients in the stress-based model (hereafter called the direct approach); (2) a regression approach to predict the nonlinear coefficients in the stress-based model (hereafter called the stress-based regression approach); (3) backcalculation of the stress-based nonlinear coefficients using the genetic algorithm (hereafter called the GA approach); and (4) the regression approach using the strain-based model (hereafter called the strain-based regression approach). For the determination of the deflections from the bare base, the nonlinear model used in backcalculation was used in forward finite element modeling (i.e., the stress-based model for (1) to (3) and strain-based model for (4)). As for the comparison with the laboratory-determined results, only the first three stress-based methods are applicable because the laboratory resilient moduli were determined as a function of stress states.

Since the deflections from only two load levels (9 and 12 kips) were available from the PCC slab testing, the ANNs presented in Chapter 4 for the direct approach could not be used. Instead, ANNs were retrained using only 9 and 12 kip data. Table 5.2 presents the RMSEs of training and testing cases for the retrained ANNs. The ANN structures with bold numbers for RMSEs were selected as the optimum structures.

For the regression approaches using the stress and strain based models, stresses and subgrade moduli at different locations on the subgrade were predicted for individual load levels. Therefore, these approaches did not require retraining of the ANNs. For the strain-based regression approach, E_{max} was predicted from the ANN trained based on 9 kip deflections. The ANN structures of 10-7-1 and 15-13-1 hidden layers in Table 4.14 were used in this field data analysis.

The GA technique was based on matching calculated deflection from a forward model against measured deflections from field FWD tests with randomly changing material properties (e.g., the PCC modulus and nonlinear coefficients of subgrade) until the error becomes smaller than the tolerance. The calculated deflections were generated by NCPAVE in the static mode using material properties randomly selected by the GA. Generally, many cases of inputs should be tried to find the material properties representing the field deflections. Finally, it was found that approximately 10 hours was necessary to obtain the coefficients within the tolerance of 10% RMSE. This run time makes the GA technique impractical for the DOT environment. More detailed information on the GA technique is given in Appendix A.

The predicted nonlinear coefficients are shown in Table 5.3 for the direct, regression, and GA approaches along with the laboratory-determined stress-based coefficients. It can be observed from the table that ANN_1 and ANN_2 are not sensitive enough to pick up the differences in the deflection basins between location A, B, and C. Thus, ANN_1 and ANN_2 were dropped from the further analysis. For the stress-based regression approach, the linearity was assumed for the deviator stress less than 0.5 psi. All of the predicted deviator stresses under 9 and 12 kip loads were less than 0.5 psi in location B. Therefore, the predicted nonlinear coefficients for location B are not available in Table 5.3.

In order to find out the reason for the low deviator stress predicted from location B, PCC modulus was investigated. From the NCHRP 10-48 study (Kim *et al.*, 2000), it was found that the surface layer modulus is a strong function of SCI. Equation (5.1) was

developed from the dynamic and nonlinear synthetic database using the regression analysis (Figure 5.4):

$$Log(Epcc) = -1.131469 * Log(SCI) - 1.695362 * Log(Hpcc) + 7.890875$$

$$(R^2 = 0.97) \qquad (5.1)$$

where

Epcc : PCC slab Young's modulus,

SCI : $D_0 - D_{12}$, and

Hpcc : PCC slab thickness.

Table 5.2 Prediction accuracy of the direct backcalculation using different input units under 9 kip and 12 kip FWD loads

Input		Hidden layer Structure	Output	Training Average RMSE (%)	Testing Average RMSE (%)
ANN_1	D_{24}, D_{36}, D_{60}, Hpcc	7-4-1	k_1	**14.49**	**9.63**
		8-5-1		14.87	10.16
		9-6-1		13.48	10.99
		7-4-1	k_3	22.10	15.87
		8-5-1		26.68	17.29
		9-6-1		**18.17**	**13.61**
ANN_2	D_0 to D_{60}, Hpcc	13-10-1	k_1	9.66	9.16
		14-11-1		**9.86**	**8.38**
		15-12-1		11.05	9.70
		13-10-1	k_3	**13.09**	**11.74**
		14-11-1		18.36	13.37
		15-12-1		23.18	16.96
ANN_3	AREA, D_{24}, D_{36}, D_{60}, Hpcc	7-4-1	k_1	13.21	10.39
		8-5-1		**9.96**	**9.13**
		9-6-1		12.16	9.69
		7-4-1	k_3	23.91	19.49
		8-5-1		18.19	16.88
		9-6-1		**21.34**	**16.40**
ANN_4	BDI, F2, D_{24}, D_{36}, D_{60}, Hpcc	11-8-1	k_1	11.81	9.43
		12-9-1		12.28	9.08
		13-10-1		**11.97**	**9.00**
		11-8-1	k_3	**17.06**	**11.64**
		12-9-1		17.73	13.85
		13-10-1		14.93	14.93

Table 5.3 Nonlinear model prediction using 9 and 12 kip load deflections of I-85 FWD tests

Backcalculation	ANN_1	ANN_2	ANN_3	ANN_4	GA	Stress-Based Regression	Strain-Based Regression	Lab Test
Input Units	D_{24}, D_{36}, D_{60}, Hpcc	D_0 to D_{60}, Hpcc	Area, D_{24}, D_{36}, D_{60}, Hpcc	BDI, F2, D_{24}, D_{36}, D_{60}, Hpcc	D_0 to D_{60}, Hpcc	D_0 to D_{24}, Hpcc	D_0 to D_{24}, Hpcc	Average of LVDT Sensors 1 & 2
Location A	k_1 = 361	k_1 = 361	k_1 = 12827	k_1 = 21846	k_1 = 5149	k_1 = 8831	E_{max} =	k_1 = 15863
	k_3 = -0.007	k_3 = -0.663	k_3 = -0.469	k_3 = -0.663	k_3 = -1	k_3 = -0.150	13,623 psi	k_3 = -0.659
Location B	k_1 = 361	k_1 = 361	k_1 = 1357	k_1 = 20820	k_1 = 19610	Linear State	E_{max} =	k_1 = 19089
	k_3 = -0.008	k_3 = -0.663	k_3 = -0.663	k_3 = -0.663	k_3 = -0.102		13,611 psi	k_3 = -0.524
Location C	k_1 = 361	k_1 = 362	k_1 = 2718	k_1 = 23139	k_1 = 17114	k_1 = 7516	E_{max} =	k_1 = 5522
	k_3 = -0.007	k_3 = -0.658	k_3 = -0.663	k_3 = -0.663	k_3 = -0.528	k_3 = -0.129	13,614 psi	k_3 = -0.304
Location D	k_1 = 361	k_1 = 362	k_1 = 13006	k_1 = 23139	k_1 = 17865	k_1 = 11125	E_{max} =	Not Available
	k_3 = -0.01	k_3 = -0.291	k_3 = -0.663	k_3 = -0.663	k_3 = -0.586	k_3 = -0.308	13,905 psi	

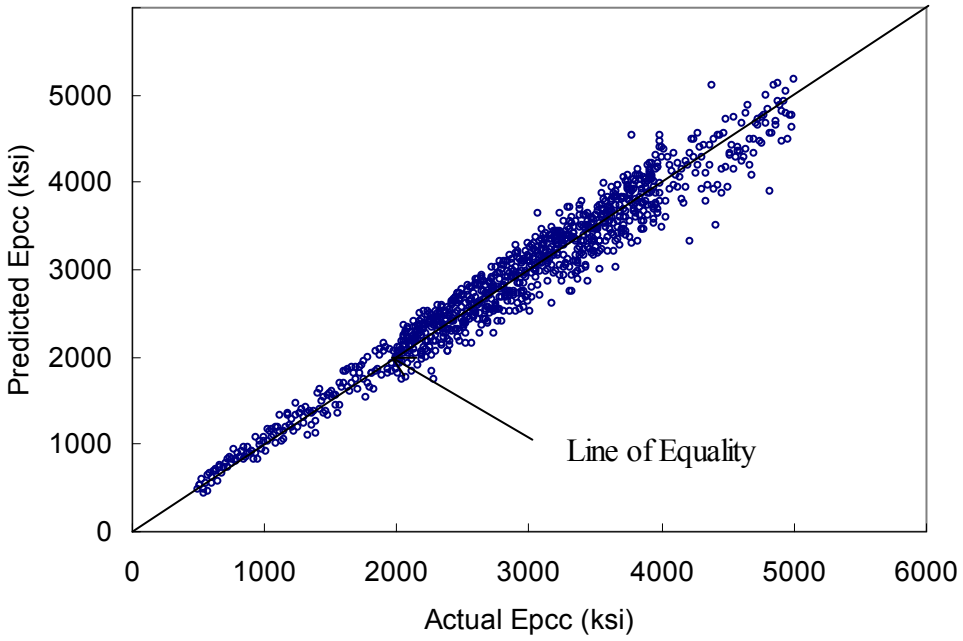

Figure 5.4 Predicted vs. actual PCC modulus

The I-85 PCC moduli were predicted using Equation (5.1) and shown in Table 5.4. The highest PCC modulus was obtained from location B, suggesting that strong PCC in location B caused the low deviator stress.

Table 5.4 Predicted PCC moduli for the four locations on I-85

Test Location	A	B	C	D
PCC Modulus (psi)	5,250,800	7,731,200	6,903,600	6,638,400

Figure 5.5 displays the subgrade moduli and deviator stresses predicted from the ANNs for the stress-based regression approach. In the case of location D, the deviator stress below the center deflection under a 12 kip FWD load showed much smaller than the deviator stress under a 9 kip FWD load. Therefore, it was necessary to exclude the data points of 12 kip FWD load in the regression analysis.

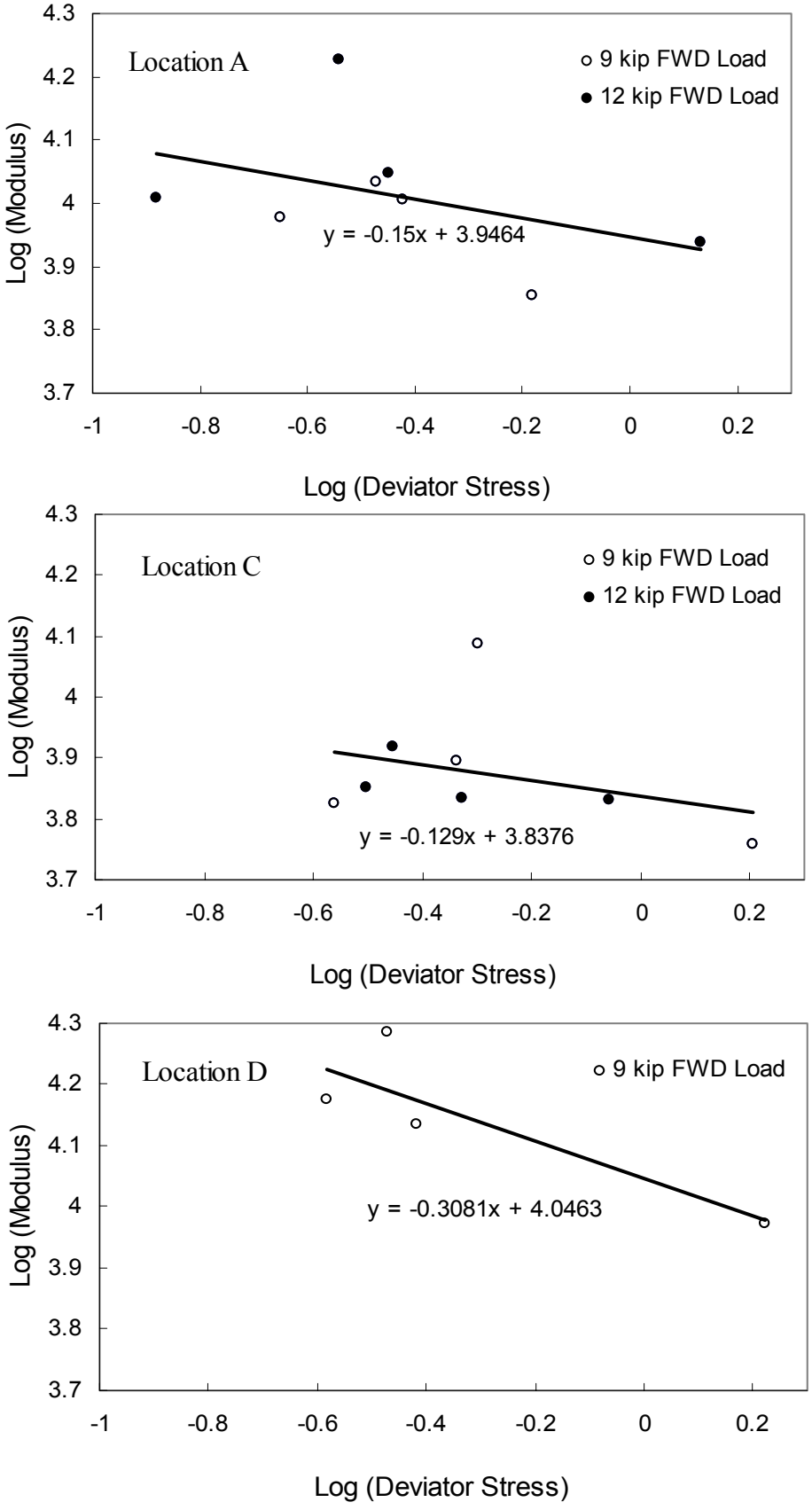

Figure 5.5 Linear regression plots from backcalculated deviator stresses and moduli

5.4 Comparison between Measured and Calculated Deflections

In this section, the different approaches (ANN_3, ANN_4, stress-based regression, GA, and strain-based regression) were tested to discern which one best predicted subgrade conditions compared to the resilient modulus lab tests of the cored soil materials. In addition, measured deflections under intact PCC slabs and bare base FWD tests were compared with calculated deflections from forward models using backcalculated nonlinear coefficients and Epcc. The backcalculated coefficients were obtained from ANN_3, ANN_4, stress-based regression, GA, and strain-based regression using FWD deflections under two load levels on PCC slabs, and the critical value of $E_{\max}$ in the strain-based regression was predicted from FWD deflections under a 9 kip load.

It needs to be noted that a discrepancy exists between the actual pavement structure and the structure used in backcalculation. The I-85 pavement has a 5-inch thick base layer, but it was necessary to neglect the base layer in the backcalculation because the ANNs were trained for two-layer systems. To be more realistic in the forward prediction, the base layer was included with a set of nonlinear coefficients estimated from the DCP results and the visual observation of the base material during the FWD tests. Figure 5.6 presents the CBR values at different depths estimated from the DCP measurements at location A of I-85. The CBR value was converted from the penetration depth measured from DCP tests according to the regression relationship in Figure 5.7. The following equation is used by the NCDOT to convert the DCP reading into the CBR value:

$$Log(CBR) = 1.563 - 1.076 * Log(DCP) \tag{5.2}$$

where *DCP* is the penetration depth (cm) at each blow.

It is observed that the CBR value of the base is not significantly different from that of the subgrade. Therefore, the base material is assumed to be cohesive because the moisture content of the base is high due to rainfall at the test sites. From Santha(1994), a coefficient set (k_1= 6967.8 and k_3= -0.366) containing a small amount of clay and silt was selected. For the strain-based approach, the normalized Young's modulus versus strain curve associated with the sand soil type (PI = 10 percent) was selected based on the findings from Kim *et al.* (1992) and Chang (1991).

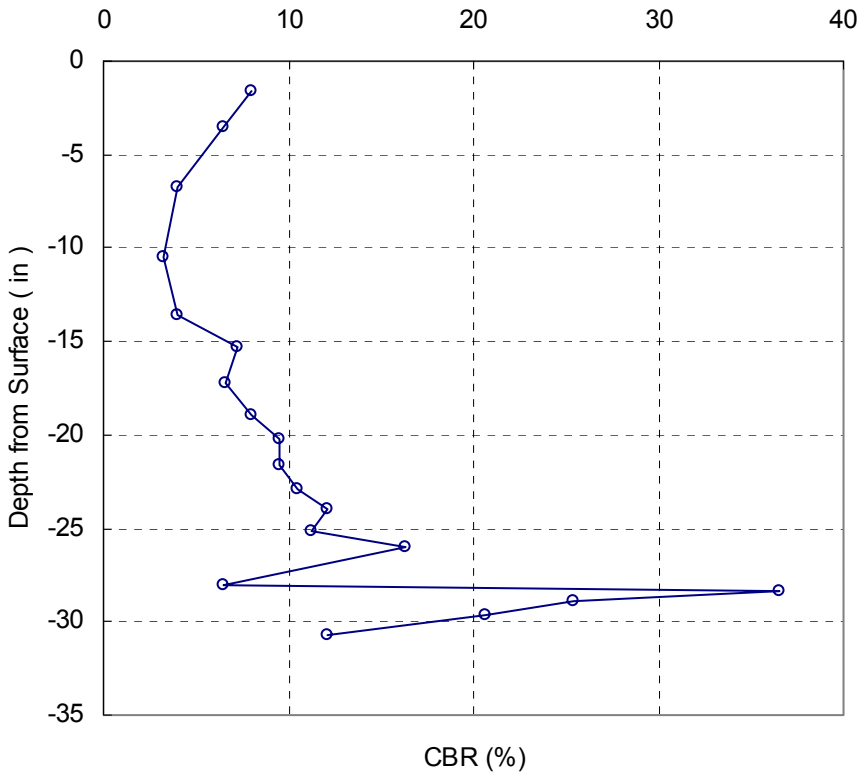

Figure 5.6 CBR vs. depth from surface at location A

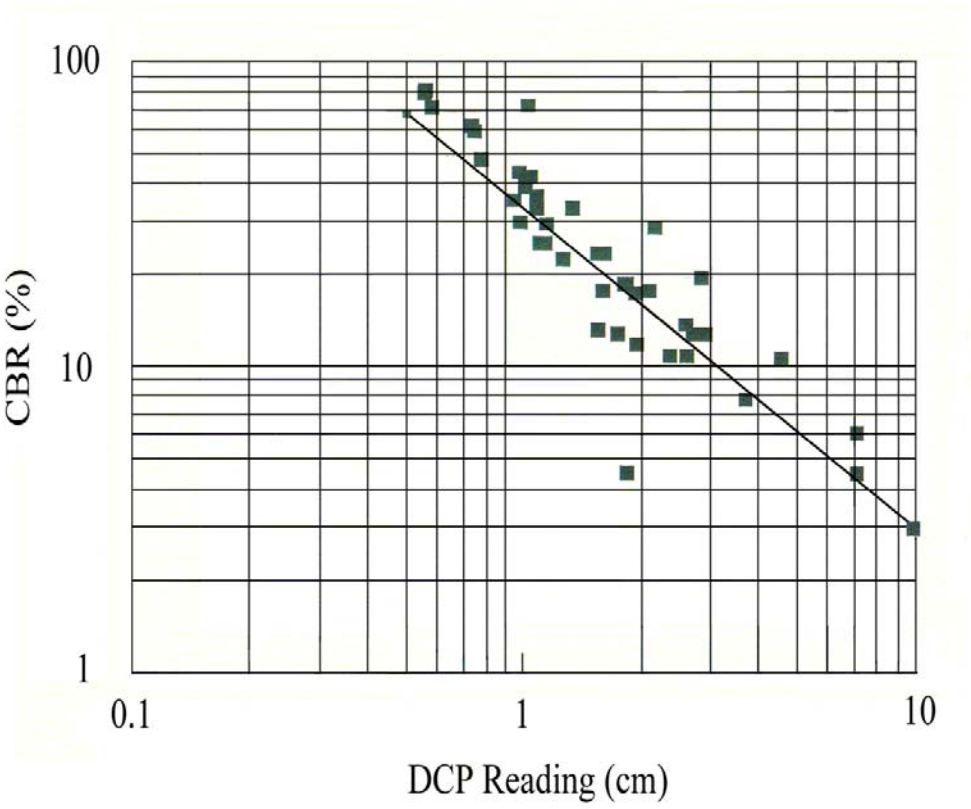

Figure 5.7 The linear relationship curve between DCP reading and CBR

Figures 5.8 to 5.10 display the deflections measured from the field tests and predicted from different backcalculation techniques. Generally, deflections predicted from the ANN_4, stress-based regression, and lab tests show good agreement with the measured deflections, considering the effects of narrowed stress distribution and rainfalls during the tests.

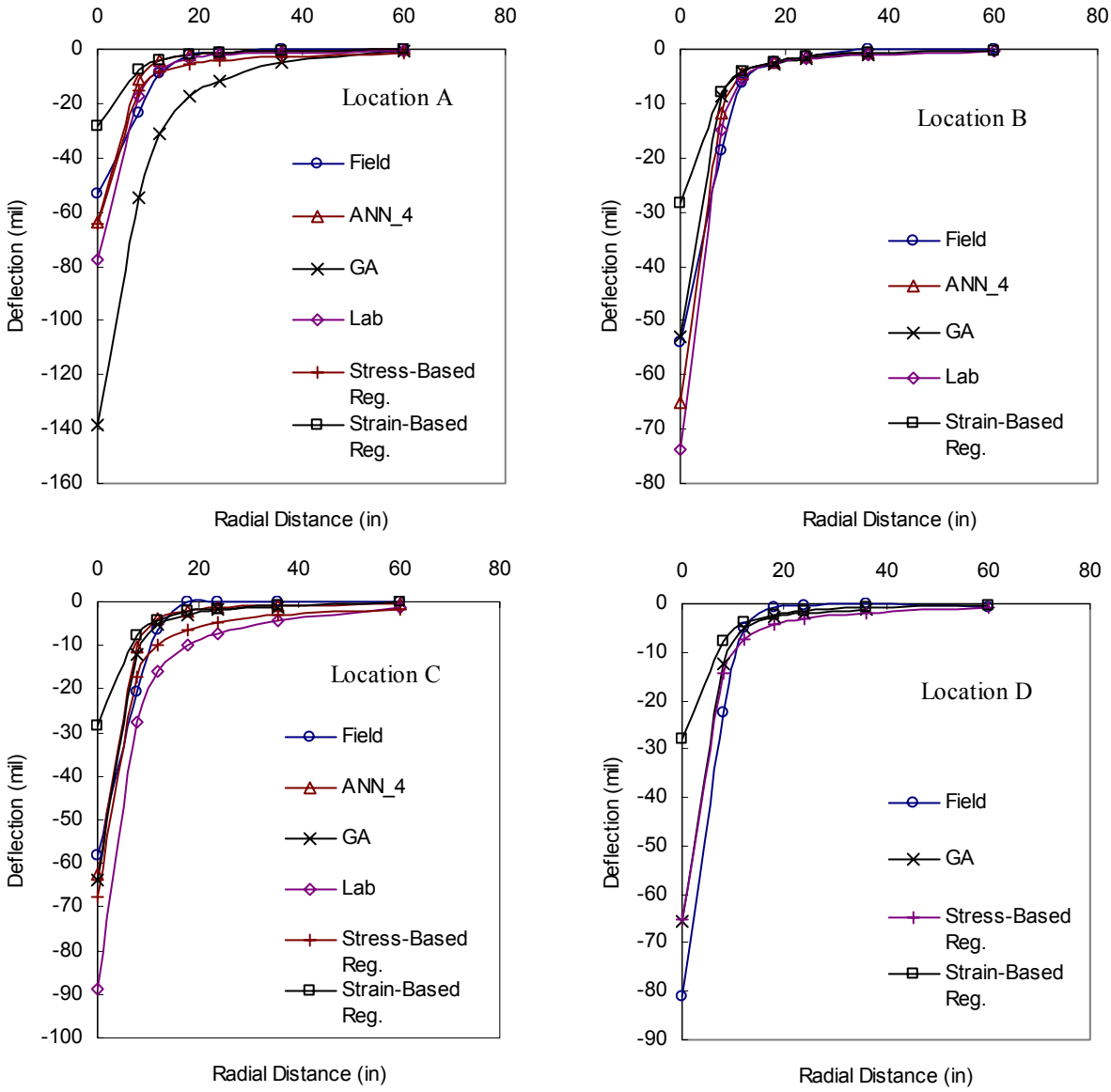

Figure 5.8 Comparison plot under 3 kip FWD load on bare base test

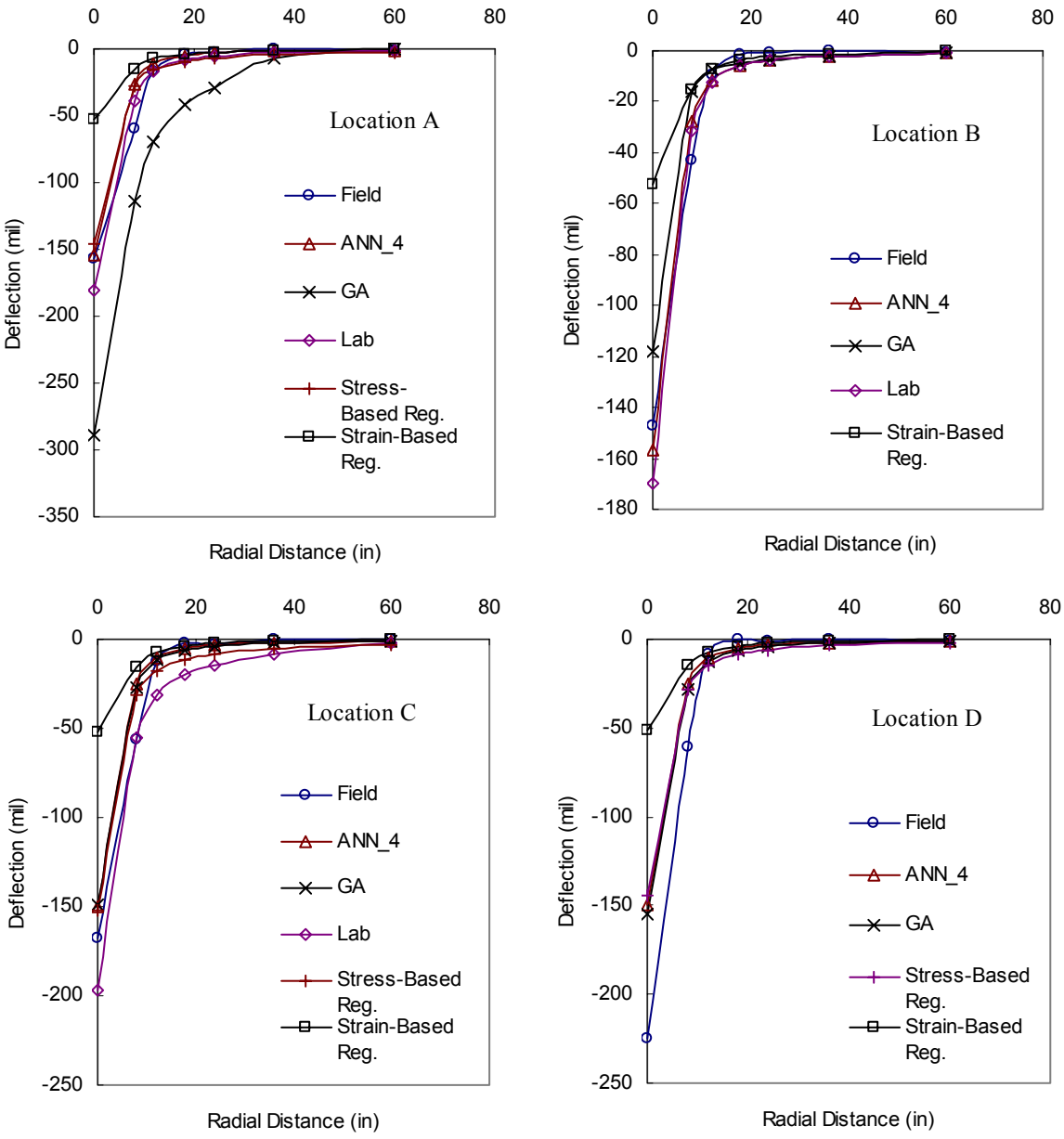

Figure 5.9 Comparison plot under 5 kip FWD load on bare base test

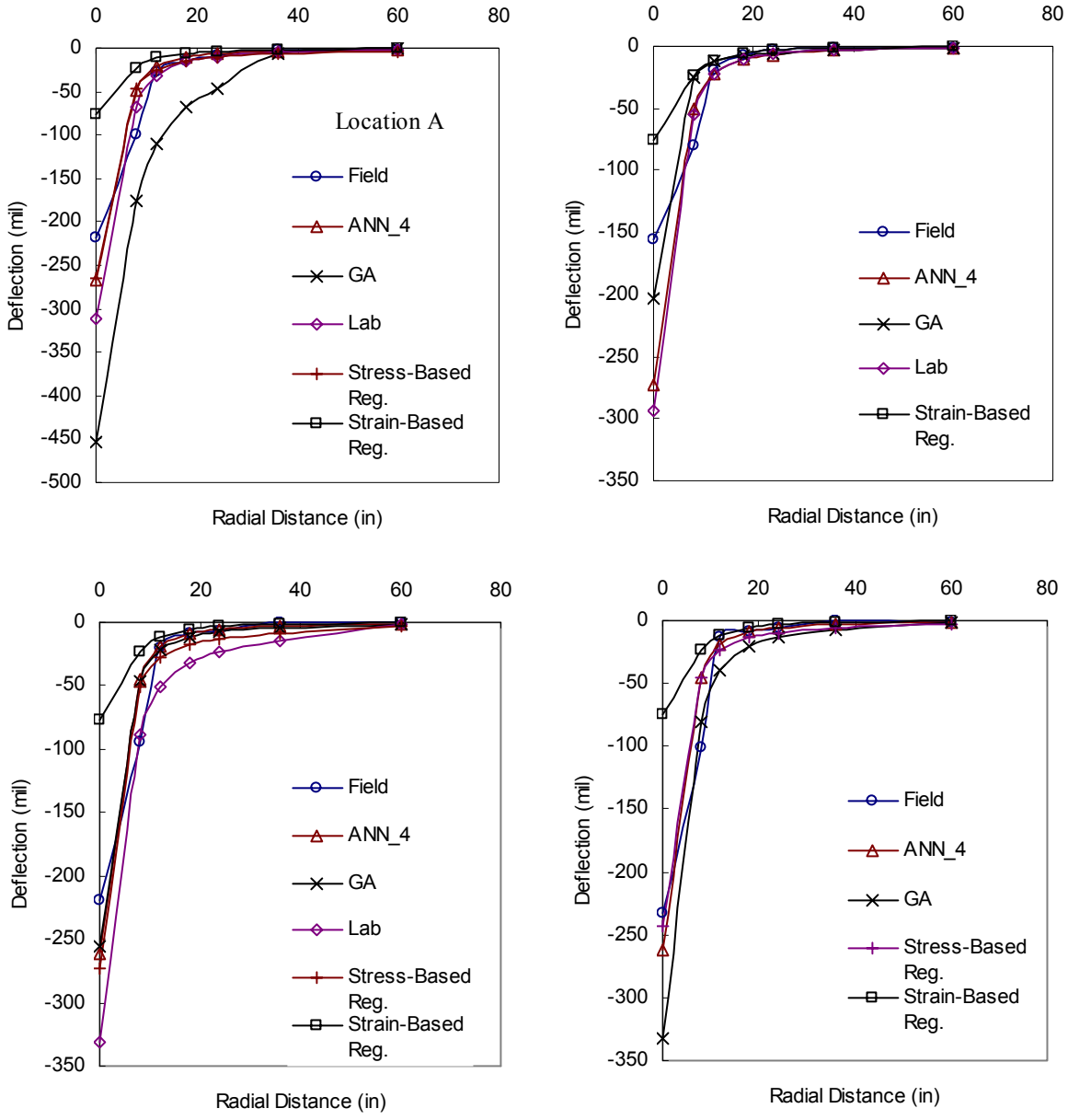

Figure 5.10 Comparison plot under 7 kip FWD load on bare base test

In Figures 5.11 to 5.13, errors between the measured and predicted deflections were plotted in these figures (denoted as Total Average Error). The error based on the prediction model of ANN_3 was not plotted due to large errors compared with the other approaches. Deflections at radial distances greater than 12 inches were not considered because the differences between calculated and measured deflections are very large in all backcalculating models. These large differences in deflections (D_{18}, D_{24}, D_{36}, and D_{60}) may be explained by a narrow stress bulb generated from FWD tests on bare base. The performance evaluation of the developed procedures is crucial to understanding the agreement between measured deflections from the bare base FWD tests and calculated deflections from the forward models based on the inputs of the predicted material properties. These material properties (Uzan's coefficients, Epcc, and $E_{\max}$) were backcalculated from the corresponding ANNs using the deflections under the multi-level loads (9 and 12 kips) on the intact PCC slabs. ANN_4 and stress-based regression approaches perform better than the lab results because the *in-situ* FWD tests neglect the effect of boring disturbance.

In general, the ANN_4, Lab, and stress-based regression approaches show lower total average errors than those from GA and strain-based regression approaches. In the GA approach, the errors in location C and D are low, but the variation in the prediction accuracy among the locations is troublesome.

In addition to the simulation of bare base response, measured deflections on intact PCC slabs were compared with calculated deflections from prediction models with estimated nonlinear coefficients.

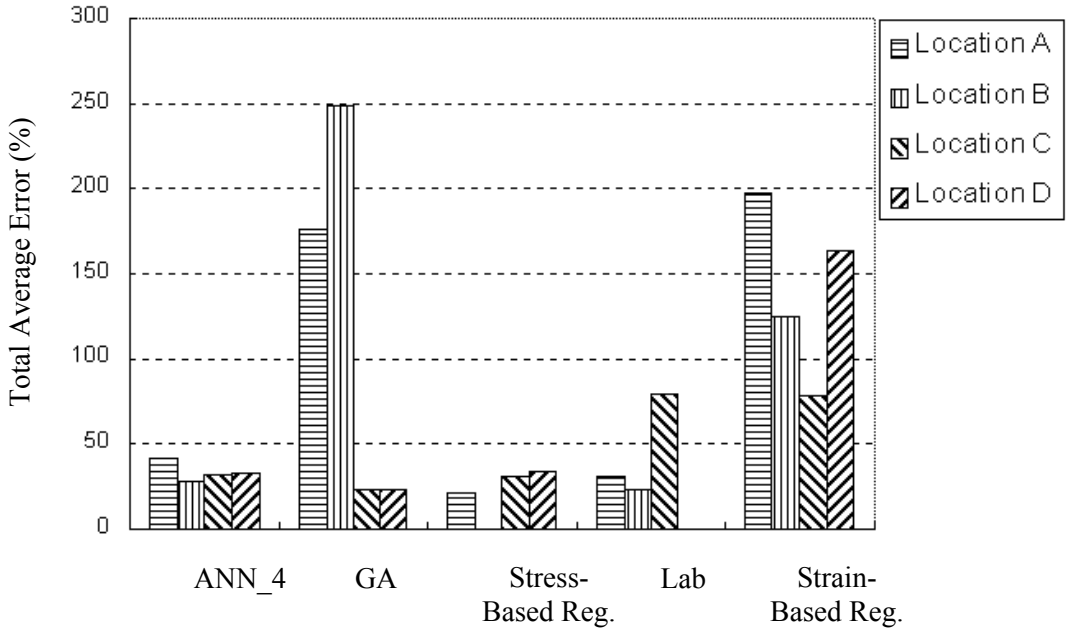

Figure 5.11 Absolute errors between calculated and measured deflections under 3 kip FWD load on bare base

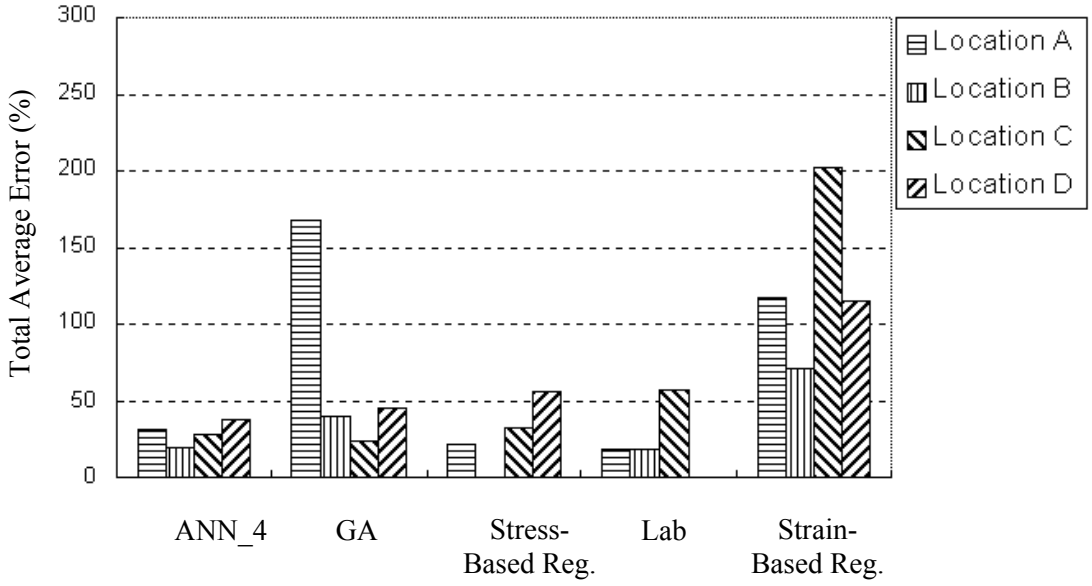

Figure 5.12 Absolute errors between calculated and measured deflections under 5 kip FWD load on bare base

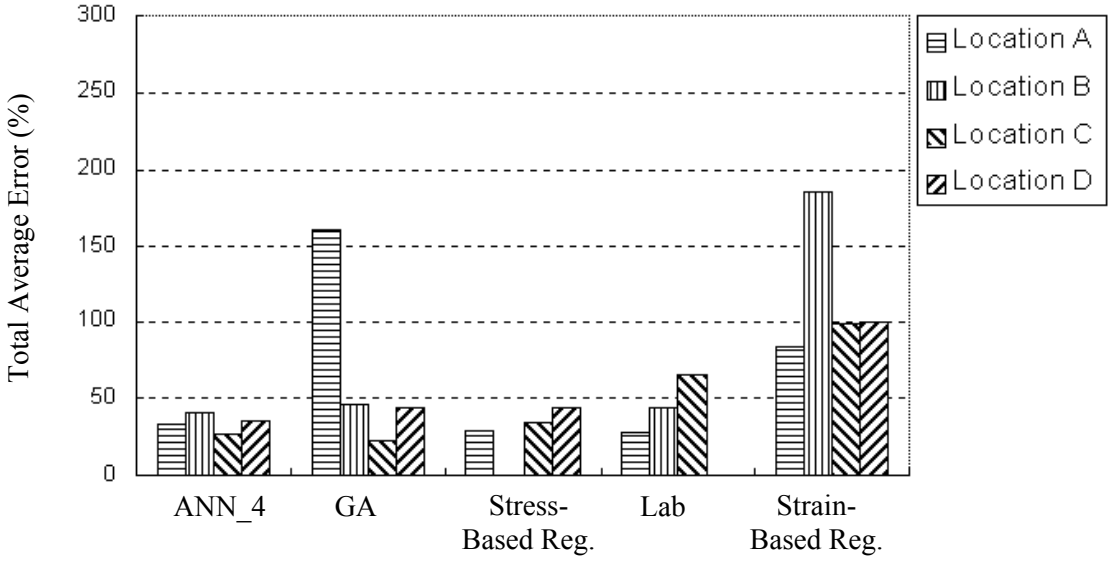

Figure 5.13 Absolute errors between calculated and measured deflections under 7 kip FWD load on bare base

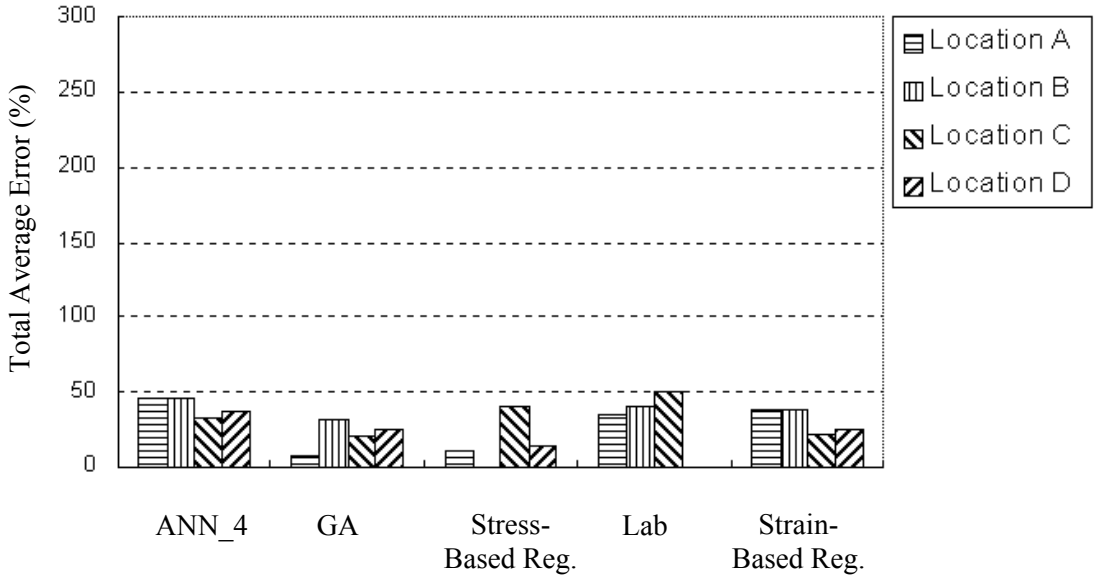

Figure 5.14 Absolute errors between calculated and measured deflections under 9 kip FWD load on intact PCC slabs

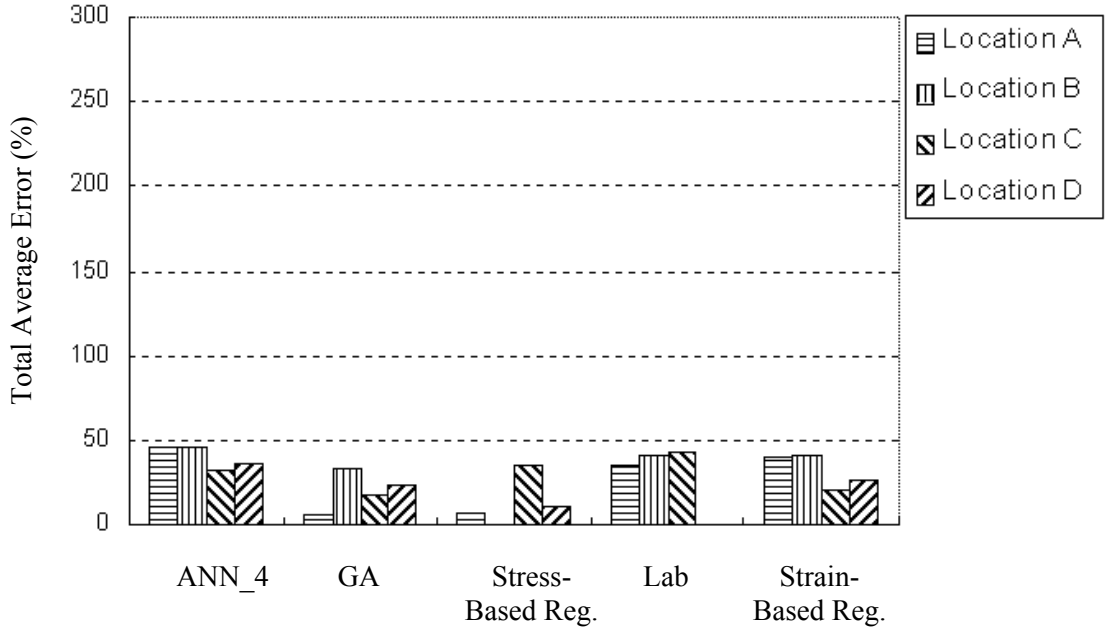

Figure 5.15 Absolute errors between calculated and measured deflections under 12 kip FWD load on intact PCC slabs

The same procedure used in the bare base response simulation was applied to the intact PCC pavement. Epcc was obtained from Equation (5.1). Figures 5.14 and 5.15 display the total average errors calculated from all seven deflections as a function of the backcalculation approach. In general, the stress-based regression and GA approaches perform better than others except location C in the stress-based regression approach. Even though the performance of GA prediction is good in this case, the implementation of this method is impractical due to the significant amount of computing time necessary to accomplish the backcalculation.

Finally, when both cases of intact PCC slabs and bare subgrade tests with varying load levels are taken into account, the calculated deflections from the stress-based regression approach in both cases show good agreement with the measured deflections

from the field tests. Based on this observation, the stress-based regression approach will be implemented to develop a backcalculation program for PCC pavements.

5.5 Recommended Procedure

The following steps are recommended to determine whether the subgrade in question is strong enough to handle a construction equipment during rubblization:

Step 1 : Conduct FWD tests at the center of intact PCC slabs using multi-level loads (9, 12, and 15 kips). To minimize the effect of warping, these tests should be performed at the earliest time in the morning.

Step 2 : Calculate the deviator stresses and moduli in subgrade at radial distance of 0, 8, 12, and 24 inches using the ANN backcalculation program.

Step 3 : Run the power regression analysis (or linear regression when logarithmic values are used) between the deviator stresses and subgrade moduli.

Step 4 : Calculate the maximum deflection caused by an equipment in question using NCPAVE-static. The input values are the predicted coefficients of the stress-based regression, the surface layer thickness, and a typical rubblized modulus of 500 ksi.

Step 5 : Determine whether the maximum deflection will cause the problems during rubblization.

CHAPTER SIX
CONCLUSIONS AND RECOMMENDATIONS FOR FUTURE RESEARCH

6.1 Conclusions

In this research, the nonlinear subgrade condition was investigated using multi-level FWD loads on intact PCC slabs. Both the stress and strain-based models were studied to represent the subgrade nonlinearity. The nonlinear coefficients in these models were determined either by presenting them directly from ANNs or by running regression analysis between stresses (or strains) and subgrade moduli predicted from surface deflections. The performance of these approaches was evaluated using the data from I-85. The following conclusions may be drawn from this investigation:

1. The nonlinearity of subgrade is important to estimate subgrade responses, such as stresses and strains, under multi-level FWD loads. The study shows that deviator stresses calculated from the nonlinear analysis are generally larger than those from the linear analysis. That is, the linear analysis could underestimate the subgrade response.
2. In general, stresses and strains in subgrade are easier to be predicted from deflection using ANNs than nonlinear material properties. Additionally, the investigation shows that in -situ FWD tests are better than destructive coring and lab test approaches.
3. Results from this study confirm that the highest FWD load on a thick and/or strong layer cannot cause nonlinear behavior in subgrade. When the predicted stress in subgrade is less than 0.5 psi, coring followed by DCP testing is recommended for subgrade stiffness evaluation.

4. Based on very limited field data from I-85, the stress-based regression approach seems to be most promising.

6.2 Recommendations for Future Research

This research has resulted in a significant amount of information regarding the subgrade nonlinearity under multi-level FWD loads. Several procedures of predicting subgrade nonlinearity under intact PCC slabs have been developed in this research using the dynamic and nonlinear synthetic database. However, the complexity involved in the nonlinear analysis requires the verification of these procedures using field data.

Only very limited data were available for this purpose during the research. It is strongly recommended to verify these procedures using additional field data in the future. The additional verification effort will require: (1) deflections measured on PCC slabs using 9, 12, and 15 kip loads; (2) deflections measured on bare subgrade using 3, 5, and 7 kip loads; (3) DCP readings; and (4) laboratory resilient moduli values of soil samples. With this additional work, a reliable backcalculation program for PCC pavement can be developed that will aid not only rubblization decisions but also the overlay thickness design after rubblization.

LIST OF REFERENCES

AASHTO. (1993). AASHTO Guide for Design of Pavement Structures. Amer. Assoc. of State Highway and Trans. Officials.

Borden, R. H., Shao, L., and Gupta, A. (1994). "Construction Related Vibrations." FHWA/NC Report 94-007, Center for Transportation Engineering Studies, North Carolina State University.

Brown, S. F. and Pappin, J.W., (1981), "Analysis of Pavements with Granular Bases." Transportation Research Record, No. 810, pp. 17-23.

Brown, S. F., Louch, S. C., and O'Reilly, M. P. (1987). "Repeated Loaded Loading of Fine Grained Soils." TRRL Contractors Report, CR72, School of Civil Engineering, University of Nottingham, Nottingham, England.

Chang, D. (1991). Nonlinear Effects on Dynamic Response of Pavements Using the Nondestructive Testing Techniques. Dissertation, UT at Austin.

Corley-Lay, Judith. (1996). NCDOT correspondence on I-85 Rubblization Project.

Corley-Lay, Judith. (1997). State Pavement Analysis Engineer. NCDOT. Personal interview.

Corley-Lay, Judith B., Thomas M. Hearne, and Shie-Shin Wu. (1995). "Deflection Study and Design of Crack and Seat Pavement Rehabilitation." Transportation Research Record, No. 1513.

Daleiden, Jerome F., David A. Ooten, and Mark D. Sargent. (1995). "Rehabilitation of a Jointed Portland Cement Concrete Pavement on I-35 (Southbound) in Kay County, Oklahoma." Transportation Research Record, No. 1513, pp. 61-69.

Dayhoff, J. (1990). Neural Network Architectures: An Introduction. Van Nostrand Reinhold, New York.

Desai, C. S., and H. J. Siriwardane. (1984). Constitutive Laws for Engineering Materials. Prentice-Hall, Inc., Englewood Cliffs, NJ.

Ellacott, S., D. Bose. (1996). Neural Networks. Deterministic Methods of Analysis, ITP, London.

Elliot, R. P., and David, L. (1989). "Improved Characterization Model for Granular Bases." Transportation Research Record, No. 1227, pp. 128-133.

Filho, J. R., C. Alippi, and P. Treleaven. (1994). "Genetic Algorithm Programming Environments. " IEEE Computer Journal, Vol. 27, pp 28-48.

Fredlund, D. G., A. T. Bergan, and P.K. Wong. (1977). "Relation Between Resilient Modulus and Stress Condition for Cohesive Subgrade Soils." Transportation Research Record, No. 642, pp. 73-81.

Garg, N., and Thomson, M. R. (1997). "Triaxial Characterization of Mn/ROAD Granular Materials." Paper presented at 76th Annual Transportation Research Board Meeting, January.

Garson, G. D. (1998). Neural Networks, An Introductory Guide for Social Scientists. SAGE Publications, London.

Goldberg, D. E. (1989). Genetic Algorithms in Search, Optimization and Machine Learning. Addison-Wesley, Reading, Mass.

Hall, K. T. and M. I. Darter. (1994). "Improved Methods for Asphalt-Overlaid Concrete Pavement Backcalculation and Evaluation." Nondestructive Testing of Pavements and Backcalculation of Moduli. 2nd Volume, STP 1198, ASTM, pp. 83-102.

Haykn, S. (1994). Neural Networks. Macmillan College Publishing Company, New York.

Hecht-Nielsen, R. (1990). Neurocomputing. Addision-Wesley. Reading, Mass.

Holland, J. H. (1975). Adaptation in Natural and Artificial Systems. University of Michigan Press, Ann Arbor.

Hylton, J. M. (1997). Rehabilitation of Aging PCC Pavement Using Rubblization Techniques. Technical Report, North Carolina State University.

Huang, Y. H. (1993). Pavement Analysis and Design. Prentice-Hall, Inc. Englewood Cliffs, New Jersey.

Iannides, A. M. (1994). "Concrete Pavement Backcalculation Using ILL-BACK 3.0." Nondestructive Testing of Pavements and Backcalculation of Moduli. 2nd Volume, STP 1198, ASTM, pp. 103-124.

Kim, D. S., and K. H. Stokoe II. (1992). "Characterization of Resilient Modulus of Compacted Subgrade Soils Using Resonant Column and Torsional Shear Tests." Transportation Research Record, No. 1369, pp.83-91.

Kim, Y. (1997). In -Situ Evaluation of Microcrack Damage and Healing of Asphalt Concrete Pavements Using Stress Wave Test. Dissertation, North Carolina State University.

Kim, Y. R., J. D. Ranjithan, J.D. Troxler, and B. Xu (2000). "Assessing Pavement Layer Condition Using Deflection Data." Final Report, NCHRP 10-48.

Kim, Y. R. and Y-C. Lee. (1997). "Condition Assessment of Flexible Pavements Using FWD Deflections." Final Report, NCDOT Project.

Kuennen, Tom. (1991). "Resonant 'rubblizing' puts asphalt over concrete." Roads and Bridges. Jan., p. 50.

Kuo, C-M., K. T. Hall, and M. I. Darter. (1995). "Three-Dimensional Finite Element Model for Analysis of Concrete Pavement Support." Transportation Research Record, No. 1505, pp. 26-32.

Lee, Y-C. (1997). Condtion Assessment of Flexible Pavements Using FWD Deflections. Dissertation, North Carolina State University.

Mallela, J., and K. P. George. (1994). "Three-Dimensional Dynamic Respons Model for Rigid Pavements. " Transportation Research Record, No. 1448, pp. 92-99.

May, R. W., and Witczak, M. W. (1981). "Effective Granular Modulus to Model Pavement Responses." Transportation Research Record, No. 810, pp. 1-9.

Michalewicz, Z. (1999). Genetic Algorithms + Data Structures = Evolution Programs. Springer-Verlag Berlin Heidelberg, New York.

NCHRP. (1996). "Laboratory Determination of Resilient Modulus for Flexible Pavement Design." National Cooperative Highway Research Board, pp.75-82.

Nelson, Thomas B., and Sam Owusu-Ababio. (1994). Preliminary Report - Research Study #93-06: Investigation of the Performance of Fractured Slab Techniques for PCC Pavements. Report for Wisconsin DOT, Oct.

Niederquell, M. G., G. Y. Baladi, and K. Chatti. (2000). "Rubblization of Concrete Pavements Field Investigation." Transportation Research Board, 79th Annual Meeting, January 9-13, Washington, D.C.

PCS. (1991). Pavement Consultancy Services. Guidelines and Methodologies for the Rehabilitation of Rigid Highway Pavements using Asphalt Concrete Overlays. Report for NAPA and SAPAE, June.

Pezo, R. F. (1993). "A general Method of Reporting Resilient Modulus of Tests of Soils, A Pavement Engineer's Point of View." Paper presented at 72nd Annual Transportation Research Board Meeting, January.

Santha, B. L. (1994). "Resilient Modulus of Subgrade Soils: Comparison of Two Constitiutive Equations. " Transportation Research Board, No. 1462, pp. 79-90.

Schackner, Bill. (1989). "Rubble rebuilds roads." The Times Union, Jan., B.

Thadkamalla, G. B., and George, K. P. (1995). "Characterization of Subgrade Soils at Simulated Field Moisture." Transportation Research Record, No. 1481, pp.21-27.

Thompson, M. R. (1999). "Hot Mix Asphalt Overlay Design Concepts for Rubblized PCC Pavements. " Transportation Research Board, 78th Annual Meeting, January 10-14, Washington, D.C.

Thompson, M. R., and Elliot, R. P. (1985). "ILLI-PAVE-Based Response Algorithms for Design of Conventional Flexible Pavements." Transportation Research Record, No. 1043, pp. 55-57.

Tutumluer, Erol, and Thompson, M. R. (1997). "Anisotropic Modeling of Granular Bases in Flexible Pavements." Paper presented at 76th Annual Transportation Research Board Meeting, January.

Uddin, W., R. B. Hackett, A. Joseph, Z. Pan, and A. B. Crawley. (1995). "Three-Dimensional Finite Element Analysis of Jointed Concrete Pavement with Discontinuities." Transportation Research Record, No. 1482, pp. 26-32.

Ullidtz, P. (1998). Modelling Flexible Pavement Response and Performance. Narayana Press, Gylling, Denmark.

Uzan, J. (1985). "Characterization of Granular Materials." Transportation Research Record, No. 1022, pp. 52-59.

Uzan, J., R. Briggs, and T. Scullion. (1992). "Backcalculation of Design Parameters for Rigid Pavements. " Transportation Research Record, No. 1377, pp. 107-114.

Waller, Fred. "Rubblizing the Raleigh Beltline." Asphalt: 8-9.

Wasserman, P. D. (1993). Advanced Methods in Neural Computing. Van Nostrand Reinhold, New York, 1993

Witczak M. W., and J. Uzan. (1988). "Universal Airport Pavement Design System. " Report I of IV , Granular Material Characterization, University of Maryland.

Yoder, E. J., and M. W. Witczak. (1975). Principles of Pavement Design. 2nd Ed. John Wiley & Sons, Inc., New York.

Zaghloul, S. M., and T. D. White. (1993). "Use of a Three-Dimensional, Dynamic Finite Element program for Analysis of Flexible Pavement." Transportation Research Record, No. 1388, pp. 60-69.

APPENDIX A
ESTIMATION OF LAYER CONDITION

One of the most important objectives in FWD testing is the estimation of pavement layer condition. To accomplish this objective, the following three elements must be present in the FWD testing and analysis:

(1) FWD testing with proper load levels and sensor spacings;

(2) formulation of a theoretical input-response relationship (that is, a forward model) from an idealized model which incorporates various parameters of assumed constitutive models for the multiple layers in the pavement system; and

(2) identification of the system parameters (that is, inversion or backcalculation) by matching *in-situ* measurements of responses and calculated responses from theoretical input-response relationships.

To accomplish the objective of this research, FWD testing with 9, 12, and 15 kip loads and sensor spacings of 8, 12, 18, 24, 36, and 60 inches was conducted. Also, a dynamic axisymmetric finite element analysis with Uzan's stress-state dependent model for subgrade was identified as an appropriate forward model. To identify the most suitable backcalculation method, various inversion techniques were examed in this research. These techniques may be categorized into the following four groups:

(1) optimization techniques in which layer moduli and thicknesses are searched (backcalculated) on the basis of error minimization strategies, such as conjugate gradient, Newton's method, and generic algorithm;

(2) data base inversion programs (e.g., MODULUS) that compare deflections with a pre-generated database to determine layer properties using interpolation;

(3) closed-form methods (Ioannides, 1994) in which a unique relationship between the deflection basin and the radius of relative stiffness is regressed to backcalculate the subgrade stiffnesses from the deflection basin parameters; and

(4) artificial neural networks in which input-output relationships are trained from a large database.

The following sections present those backcalculation techniques that are considered candidates in this research.

A.1 Existing Backcalculation Methods for Rigid Pavement

A.1.1 Theoretical Models for Backcalculation

In this section, three types of models are presented for evaluating the material parameters in the rigid pavement. These models have linear load-deformation characteristics and cannot represent any nonlinear material behavior or discontinuity between each layer. Most PCC forward models have been developed based on these theoretical models when PCC pavement structures are assessed. Some modified programs consider PCC slab curling effect due to temperature cycling.

A.1.1.1 Hertz-Westerggard Model

In this model a concrete slab rests on a dense liquid foundation, which is composed of an infinite number of springs. The total volume of displacement of the foundation is proportional to the total applied load. Based on this relationship, the modulus of subgrade reaction and the radius of relative stiffness in the slab-subgrade system may be determined. Since the vertical force at a given spring depends only on the

vertical deflection at that spring and is independent of the deflections at all other points, the liquid foundation does not simulate the actual field condition.

A.1.1.2 Hogg Model

The Hogg model represents the pavement with infinite concrete slab resting on an elastic foundation. An elastic foundation behaves more realistically than a liquid foundation because the deflection depends not only on the force at a given point but also on the forces at all points. (Huang, 1993). This type of foundation is also called a Boussinesq foundation because the Boussinesq equation for surface deflection is used for determining the stiffness matrix. In this model, the pavement parameters are the subgrade modulus of elasticity and the radius of relative stiffness of the slab-subgrade system. The load-deflection relationship is defined as follows:

$$w_{i,j} = \frac{P_j(1-\nu_f^2)}{\pi E_f d_{i,j}} \qquad \text{(A.1)}$$

where

w = deflection at given node,

P = force at given node,

E_f = elastic modulus of foundation,

d = distance of nodes, and

ν_f = Poisson's ratio of foundation.

A.1.1.3 Multi-layered Elastic Model

This model, usually used in flexible pavement, assumes Hooke's model to characterize the linear elastic layers. The linear elastic layers extend to infinity in the horizontal direction.

A.2.1 Backcalculation Procedures

A.2.1.1 JUSLAB Procedures

The JUSLAB, proposed by Uzan *et al*. (1992), is the one method used to determine the material parameters using FWD deflection data in the rigid pavement. This backcalculation procedure of layer properties for rigid pavement follows the MODULUS backcalculation framework. The outputs are the set of layer moduli that minimize the error between measured and theoretical calculated deflection bowls.

(1) A linear elastic computer program is run for a range of layer moduli, and the resulting deflections are stored in a deflection database.

(2) Pattern search and interpolation schemes are used to minimize the error between measured and theoretically calculated deflection bowls.

In order to minimize error, a pattern search routine to find the layer moduli uses an objective function as follows:

$$\min \sum_{i=1}^{N} \left[\frac{\left(D_{mi} - D_{ci}\right)}{D_{mi}} \right]^2 \qquad \text{(A.2)}$$

where

D_m = the measured deflection,

D_c = the calculated deflection, and

N = the total number of sensors.

A.2.1.2 ILLI-BACK Procedures

The backcalculation scheme described in the ILLI-BACK program employs a closed-form method that allows a choice from among several popular plate-sensor arrangements, involving the 11.81 or 17.71 in diameter plate, with four or seven sensors, as well as the irregular sensor space (Ioannides, 1994). In general, the deflections at four sensors with distances of 0, 12, 24, and 36 in (D_0, D_{12}, D_{24}, and D_{36}) from the center are measured to calculate the deflection parameter called AREA. The AREA is used to determine a radius of relative stiffness, l, depending upon the application to a concrete slab on a dense liquid or elastic solid foundation. The relationship between AREA and l is defined by theoretically representative equations. The radius of relative stiffness, l, may easily be determined by the graph of AREA variation with l (Figure A.1).

All three of the values (AREA, l, and load plate radius (a)) are expressed in units of length (inches). Now, AREA and the radius of relative stiffness are calculated as follows:

$$\text{AREA}=6\left[\frac{D_0+2D_{12}+2D_{24}+2D_{36}}{D_0}\right] \tag{A.3}$$

where

D_i denotes the deflection with the distance of i .

$$\text{For the dense liquid foundation: } l=l_k=\sqrt[4]{\frac{Eh^3}{12(1-\mu^2)k}} \tag{A.4}$$

For the elastic solid foundation : $l = l_e = \sqrt[3]{\frac{Eh^3(1-\mu_s^2)}{6(1-\mu^2)E_s}}$ (A.5)

where

E = slab Young's modulus,

E_s = soil Young's modulus,

h = slab thickness,

μ = slab Poisson ratio,

μ_s = soil Poisson ratio, and

k = modulus of subgrade reaction.

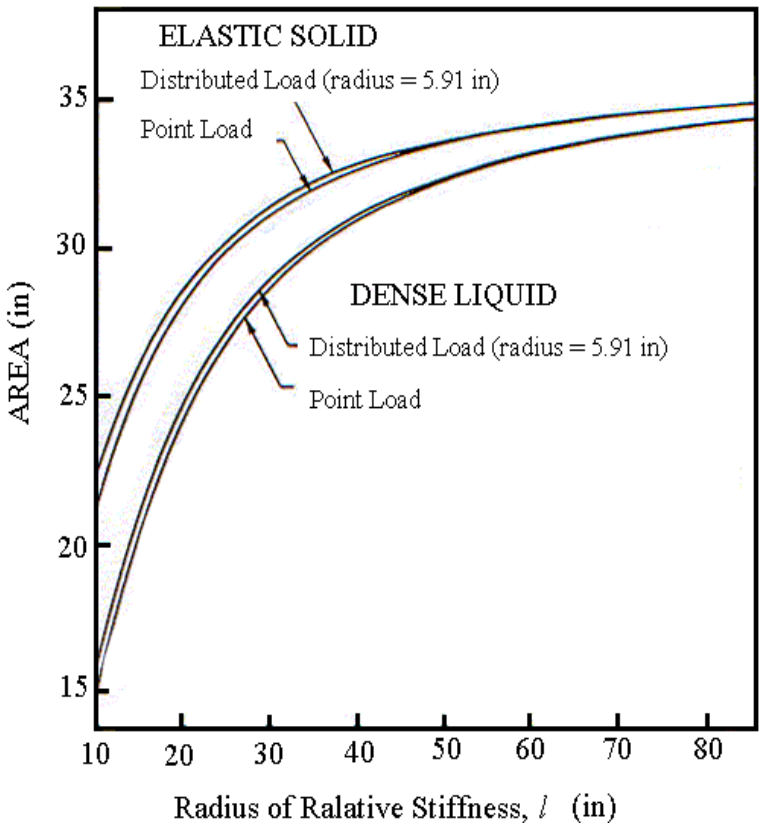

Figure A.1 Variation of AREA with l (Ioannides, 1994)

As seen in Equation A.4, the dense liquid foundation cannot be applied when determining a subgrade modulus. Therefore, the backcalculation procedure using the elastic solid foundation model must be explained in detail. For elastic solid foundations, nondimensional deflections (d_i) can be expressed as

$$d_i = \frac{D_i D}{Pl^2} = f_i\left(\frac{a}{l}\right) \tag{A.6}$$

where

D_i = deflection with the distance of i,

a = radius of load plate, and

D is the slab flexural stiffness, which is given by :

$$D = \frac{Eh^3}{12(1-\mu^2)} \tag{A.7}$$

According to studies (Ioannides, 1984; 1988), the nondimensional deflections, d_i can all be written as functions of $(\frac{a}{l})$ only. The functional form of $f_0(a/l)$ is provided by Losberg's solution for the deflection at the center of the load.

$$f_o(a/l) = \frac{1}{3\sqrt{3}}\left\{1-(\frac{a}{l})^2[0.141335-010340\ln(\frac{a}{l})]\right\} \tag{A.8}$$

Curve-fitting techniques were used in the ILLI-BACK program to obtain the regression equation for $f_i\left(\frac{a}{l}\right)$ (for i=1, … , n). From the known load plate radius, a, the

nondimensional deflection may be obtained by the regression equation or a relationship graph between nondimensional deflections and radius of relative stiffness. Therefore, the foundation elastic subgrade modulus can be backcalculated from Equations 4.5 to 4.7 as follows:

$$E_s = (1-\mu_s^2)\frac{d_i}{D_i}\frac{2P}{l} \tag{A.9}$$

Additionally, the slab flexural stiffness and the slab modulus can be calculated and expressed respectively as:

$$D = \frac{Eh^3}{12(1-\mu^2)} = \frac{d_i}{D_i}Pl^2 \tag{A.10}$$

$$E = \frac{12(1-\mu^2)}{h^3}\frac{d_i}{D_i}Pl^2 \tag{A.11}$$

On the basis of the fundamental concept above, the backcalculation procedure may be applied along the following steps:

(1) Carry out FWD tests, and record the applied load as well as the measured deflections.

(2) Calculate the deflection parameter called AREA.

(3) Determine the radius of relative stiffness, l, using the calculated AREA from the relationship curve.

(4) Determine the nondimensional deflection with the l value from a graph showing the relationship between l and d_i.

(5) Based on l and d_i, compute E_s, D, and E.

A.2.1.3 RMODS Program

Uzan *et al.* (1992) developed RMODS (rigid pavement evaluation and backcalculation system) that is based on the pattern search technique for matching the measured deflection basin with a theoretically calculated deflection basin. The procedure for backcalculating the pavement parameters is similar to MODULUS for evaluating flexible pavements. RMODS analyzes deflection basins with the corresponding theoretical forward model as follows:

(1) For the edge deflection basins, only the Westergaard model is used since all other models are not applicable.

(2) For center slab deflection basins, either the Hertz or the multi-layer elastic models is used.

A.3 Base Damage Index and Shape Factor F2

Kim *et al.* (1997) investigated relationships among deflection basin parameters, layer moduli, and layer thicknesses. They found that the relationship between Base Damage Index (BDI) and Shape Factor F2 is uniquely defined for each value of E_{sg} and is independent of upper layers' moduli and thicknesses. The BDI and F2 are defined as:

$$BDI = D_{12} - D_{24} \tag{A.12}$$

$$F2 = \frac{D_{12} - D_{36}}{D_{24}} \tag{A.13}$$

where

BDI = Base Damage Index (mil),

F2 = Shape Factor (dimensionless),

D_{12} = deflection at distance 12 in from center of load plate,

D_{24} = deflection at distance 24 in from center of load plate, and

D_{36} = deflection at distance 36 in from center of load plate.

Field measurements from different pavements are plotted in Figure A.2 along with the ABAQUS results. The data from these pavements represent deflection measurements at different times of day and at four different seasons. Although the trend is not as clear for the ABAQUS data due to the seasonal effect, the same conclusion drawn from the computed data may be drawn also for the field data. This finding is quite useful because the effect of the changing condition of the surface layer on the subgrade modulus is minimized. Another advantage of this approach is that it is applicable to distressed pavements as well as intact ones.

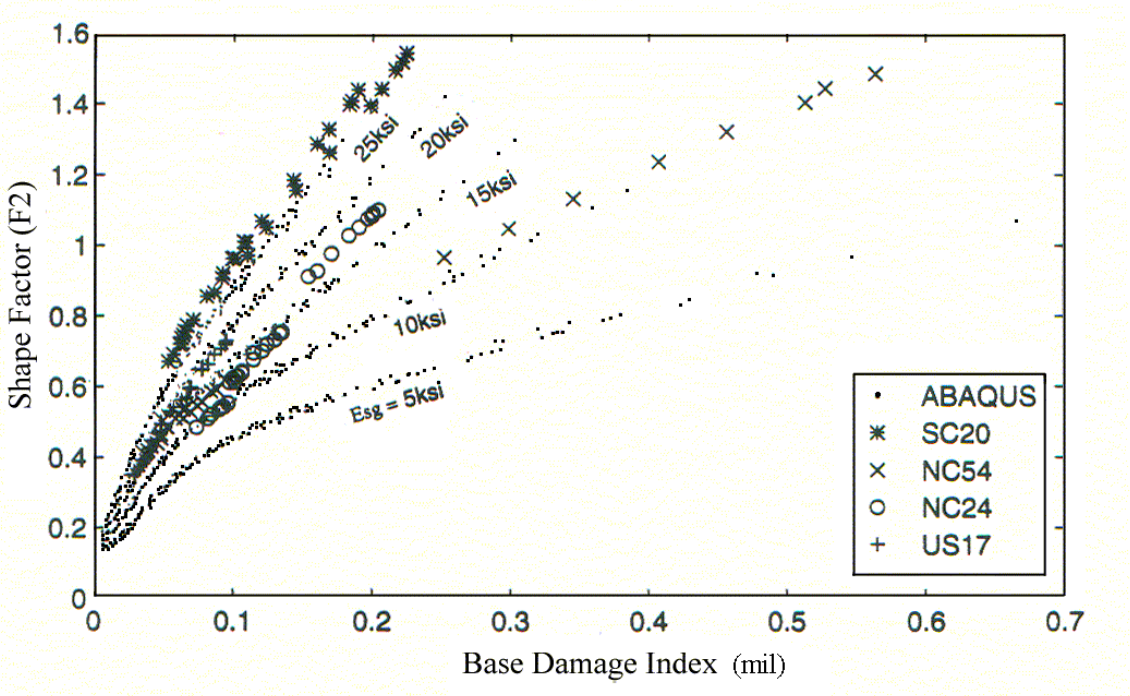

Figure A.2 Characteristic trends between F2 and BDI for identifying subgrade stiffness independent of upper layer condition.

A.4 Artificial Neural Networks

Artificial neural networks are a computational paradigm completely different from conventional serial computing. Instead of the linear sequence of relatively complex tasks that typifies most mathematical algorithms, artificial neural networks process information in parallel using a large number of operationally simple but highly interconnected processing units. The processing units have certain functional similarities to biological neurons, and their organization bears resemblance to the organization of neurons in the brain (Wasserman, 1993).

A neural network is a massively parallel distributed processor that has a natural tendency for storing experiential knowledge and making it available for use. It resembles the brain in two respects:

(1) Knowledge is acquired by the network through a learning process.

(2) Inter-neuron connection strengths, known as synaptic weights, are used to store the knowledge (Haykin, 1994).

Neural network approaches are inspired, therefore, by biological neural networks. It is generally understood that all biological neural functions, including memory, are stored in the neurons and in the connections between them during a learning process. As Figure A.3 illustrates, in biological neural networks dendrites collect signals which they feed to the neuron. The neuron, in turn, processes the signals by sending a spike of electrical current along an axon, discharging it at a synapse connecting it to other neurons, which in turn are excited or inhibited as a result. In an artificial neural network, input signals are sent to a neural processing entity, also called a neuron. After processing, the neuron sends an output signal on to other neurons in the network (Garson, 1998).

Therefore, a neural network is a parallel distributed processing system composed of processing entities (generally called neurons or units) that are interconnected to form a mathematical representation of the mapping or relationship that may be embedded in any set of data. The structure of ANNs allows the processing entities to be global approximators even in the absence of knowledge about the mathematical form of the mapping between an input signal and the corresponding output signal. A multi-layer feedforward network is the most common class of ANNs used for this type of function mapping (Dayhoff, 1990).

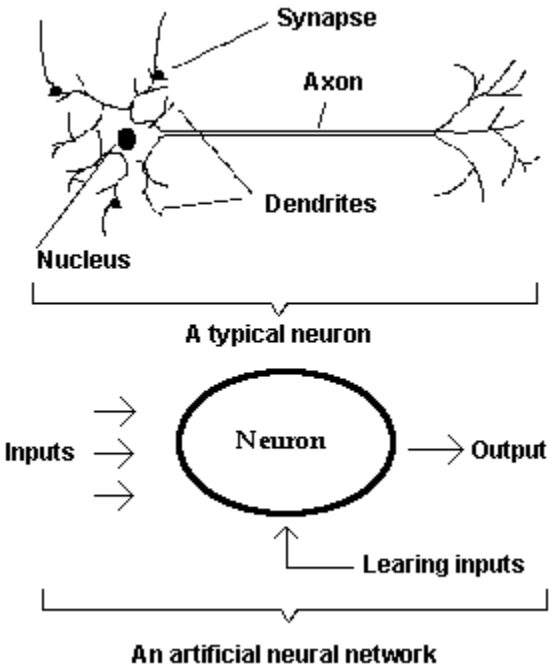

Figure A.3 Biological and neural networks

A typical multilayered network is characterized by the presence of one or more hidden layers, whose computation nodes are correspondingly called hidden units or

hidden neurons (Figure A.4). The function of the hidden units is to intervene between the external input and the network output (Haykin, 1994). The input signal is presented to the network through the units in the input layer. This signal is then propagated through the hidden units to the output units via the interconnections in the network. The strength of the propagated signal is adjusted throughout the network by the connection strengths, generally called weights. These weights are updated, in an iterative manner, until the predicted output signals are as close as possible to the actual signals corresponding to those input signals (Hecht-Nielsen, 1990).

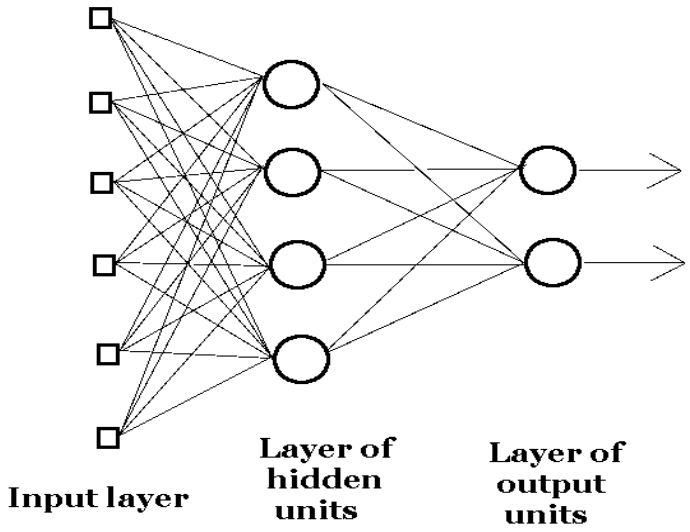

Figure A.4 Typical multilayered network with one hidden layer and output layer

A representative sample data set that includes a set of input signals and its corresponding output signals is used during this weight updating process. This process is called training. This trained network is then able to propagate a new input signal through the network and predict the resulting output signal. In this mode of operation, the network

is used as an approximate function of the mapping between the input and the output signals. Dayhoff (1990) and Hecht-Nielsen (1990).

In the feed-forward type network, the ANN is trained to capture the mapping or relationship between deflection basins as input signals and the corresponding pavement characteristics (e.g., subgrade condition) as output signals. The database, combined with many pavement characteristics and deflection basins calculated from a forward model, are used to train the ANN that yields the relationship with the result of updated weights. Based on the resulting weights, measured deflection basins from *in-situ* FWD tests are presented to the network in order to backcalculate structural layer conditions.

A.5 Genetic Algorithm Optimization Technique

A genetic algorithm (GA) is a computational model inspired by evolution to solve problems in a wide variety of domains. A GA is particularly suitable for the solution of a complex optimization problem and a non-gradient-based, probabilistic global search procedure that is designed based on the survival-of-the-fittest phenomenon prevalent in natural evolution (Holland, 1975).

A GA comprises a set of individual elements (the population) and a set of biologically inspired operators defined over the population itself. According to evolutionary theories, only the most suited elements in a population are likely to survive and generate offspring, thus transmitting their biological heredity to new generations (Filho, 1994). In computing terms, a GA program consists of the following key operations: creation of a population of strings, evaluation of each string, selection of the best strings, and genetic manipulation (crossover and mutation). These operations

represent a cycle that is repeated until an error is within a tolerance range. Figure A.5 shows these four steps. At the first step, an initial population of potential solution is randomly generated as a starting point. In the next step, the fitness (or performance) of each individual of the population is evaluated with respect to the constraints of the problem or a matching between measured deflections and calculated deflections. Based on the result of the individual performance, a selection process chooses a good genetic set to be manipulated with respect to crossover and mutation.

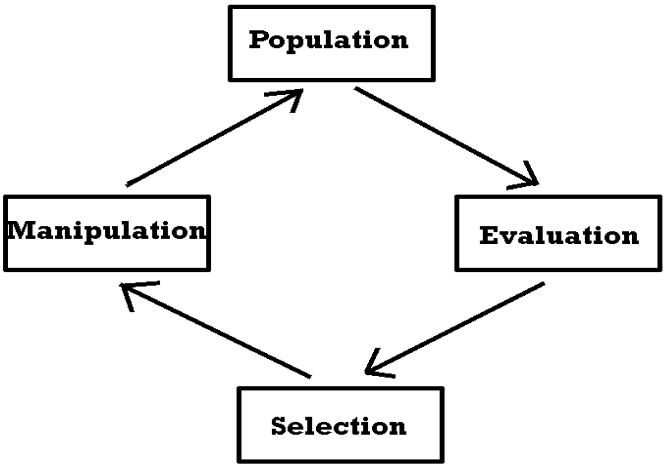

Figure A.5 Genetic algorithm cycle

The crossover operation is performed in a random manner to take chromosomes (that is, surviving input data derived from matching evaluation between measured deflections and calculated deflections), exchange part of their embedded information, and produce new chromosomes. The mutation is implemented by occasionally altering the information at randomly selected locations. The offspring (that is, new input data as the

set of the next population) generated by the genetic manipulation process provides the next population to be evaluated. This generating population-selection-evaluation-manipulation cycle is repeated in an iterative manner until a satisfactory solution (that is, the reasonable solution of matching the *in-situ* measured deflections) to the problem is found.

Figure A.6 shows the structural parameters (that is, layer thicknesses and moduli) as the GA population is randomly selected to undergo the evaluation (or fitness) that carries out matching the measured deflections from *in-situ* FWD tests and the calculated deflections from a forward model. Some data of the calculated deflections survive because their basins have fewer errors than others do with respect to the fitness process. In the next step, these data are transferred to a mating pool to sequentially perform crossover and mutation, thus generating updated population. This cycle is repeated until the population converges to the set of pavement parameters that minimize the error.

The GA process provides the advantage of simple application in that it does not require any gradient information during the error minimization. Therefore, any numerical forward model may be used in the GA. Unlike gradient techniques, this algorithm searches the error of a global point, and the best solution does not depend on initial values.

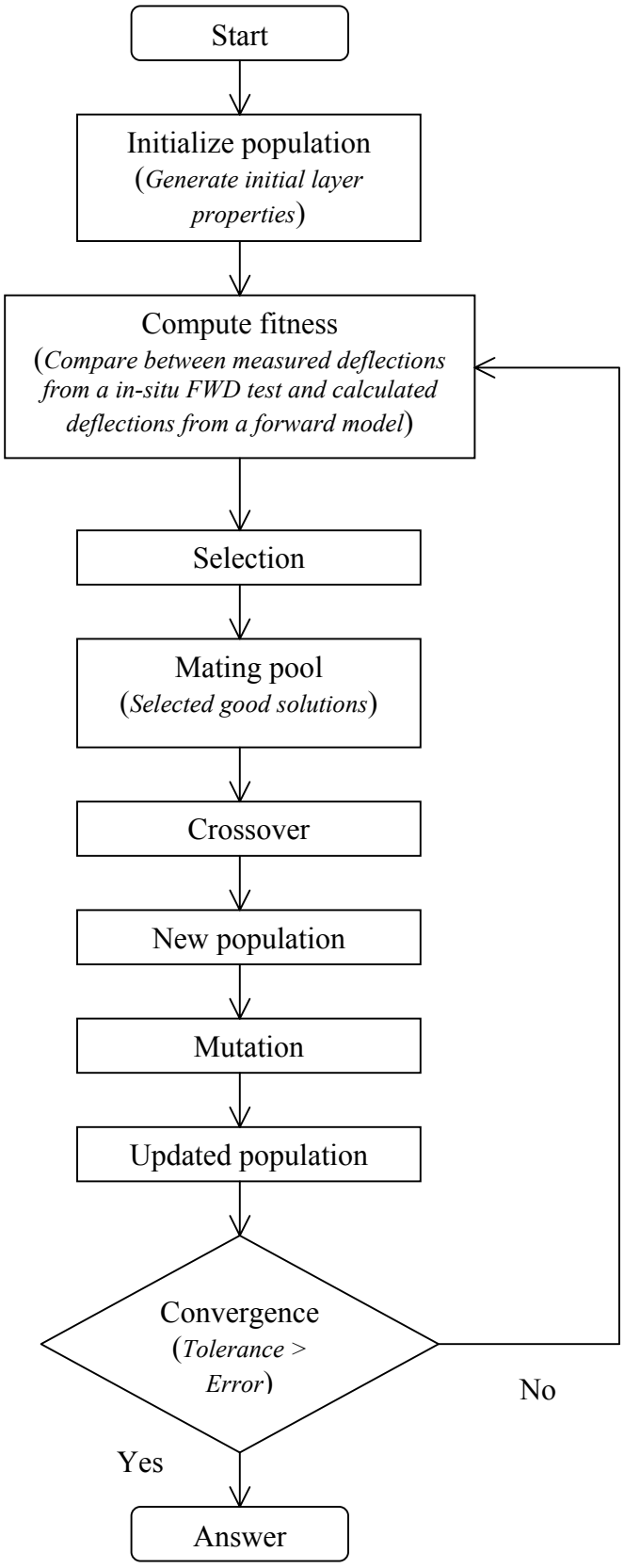

Figure A.6 Schematic diagram of genetic algorithm techniques